

---

# 50: Estimation of the Surface Energy Balance

**ZHONGBO SU**

*International Institute for Geo-Information Science and Earth Observation (ITC), Enschede, The Netherlands*

*Radiation and latent and sensible heating are among the most important processes in land–atmosphere exchanges. Hence, quantitative understanding and accurate estimation of these fluxes at large scales are imperative for research and applications in areas ranging from numerical weather forecast, climate research, water cycle study, to water resources management, sustainable agricultural production, and ecological conservation. Quantitative remote sensing is probably the only efficient and economically viable technology to provide regional to global radiometric observations of several physical quantities that are relevant to the estimation of these fluxes. This article examines the physical principles underlying the radiation and turbulent heating, along with exploring the possibilities and difficulties for estimation of these fluxes using remote sensing measurements. Past efforts, recent progresses are reviewed, and future research needs are identified. In particular, the Surface Energy Balance System (SEBS), recently developed in Wageningen, is introduced and its strengths and weakness are analyzed in view of future space-borne sensor systems. Several applications derived on the basis of SEBS, including estimation of turbulent heat fluxes, evaporative fraction and actual evaporation, estimation of relative soil moisture, and drought monitoring are discussed.*

## INTRODUCTION

The international environmental sciences communities have seen a very rapid evolution over the last years. A new global, interdisciplinary science of the Earth System has emerged at the interface of science and policy development. The need to bridge, in a more focused way, the gap between earth sciences and sustainable management of the terrestrial environment is already emerging as an overall priority both in the International Geosphere Biosphere Programme (IGBP) and the World Climate Research Programme (WCRP) (e.g. Kabat, 1999). In this regard, understanding the interactions between terrestrial ecosystems and the atmosphere is essential to address issues such as climate change and environmental degradation. Extensive scientific investigations over the past decades have demonstrated beyond doubt that the biosphere is tightly coupled to its physical environment over a wide range of space and timescales and the atmospheric circulation is strongly influenced by land surface properties and their variability in space and time. Since radiation and turbulent heating are among the most important processes in

land–atmosphere exchanges, accurate estimation of these fluxes at large scales is imperative for research and applications in areas ranging from numerical weather forecast, climate research, water cycle study, to water resources management, sustainable agricultural production, and ecological conservation. Such importance may be viewed in the following context. In dealing with climate–land interactions – especially in studies concerning terrestrial water, energy, and carbon cycles, models are often used to assist urgent policy decisions on environmental issues – but we must ask the following questions before the results derived from such models being used for further decision-making processes:

Is the interaction with a dynamic terrestrial biosphere in global models properly understood so that our forecasts of the long-term evolution of climate are reliable?

Are processes at scales from global to local properly linked so that our assessment of the impacts of climate variability on land and water resources is reliable and scenarios on the evolution of the terrestrial biosphere are realistic?

Are the political decisions based on the current model simulations/predictions/scenarios well founded?

To be able to answer these questions, there is a critical need to understand the feedbacks between the land surface and the atmosphere at various scales (Wood, 1998). As shown by recent works, the land component of the climate system must be viewed as an active participant in the coupled system, rather than a passive recipient of atmospheric forcing (Entekhabi *et al.*, 1999; Koster *et al.*, 2000). In this view, accurate representation of land surface dynamics is more important than it had been thought previously. It has also been suggested that, in the 2001 Intergovernmental Panel on Climate Change (IPCC) report, the role of land surface in modifying the climate has not been adequately considered and the effects of land-cover change on climate may be comparable to, and, perhaps larger than, the effects on climate due to changes in atmospheric composition. The current level of scientific understanding in land-atmosphere interactions has been characterized as “very low” (Pielke, 2001a, b). A recent study by Kalnay and Cai (2003) clearly shows that the impact of land use on climate change has been underestimated. Further, the current parameterizations of land processes in all earth system models are based on simple conceptions that are representative, at best, of homogeneous flat land surfaces, and few observation data sets over complex terrain exist to allow integrated long-term off-line testing that is essential to evaluate land surface parameterizations in climate models. Abilities to estimate radiation and turbulent heat fluxes using radiometric measurements from satellite sensors will help to resolve the above-mentioned uncertainties and difficulties.

Several land-atmosphere exchange processes can be distinguished in terms of exchanges of radiation, heat, water, and carbon, and other gasses. More specifically, we may consider: solar radiation, thermal radiation, sensible heat flux, latent heat flux including phase change, soil heat flux and advection, precipitation, water and vapor transport in soil, as well as biochemical processes in soil and canopy. The driving forces of these processes are solar radiation and wind. Since most of these processes vary continuously in space and time from local to global scale, and from seconds to decades and centuries, their adequate quantification also requires measurements with corresponding spatial-temporal coverage. It is in this aspect that remote sensing can play an essential role. In the following, we will briefly review some progress made in the estimation of turbulent heat fluxes.

## A BRIEF HISTORY IN REMOTE SENSING OF TURBULENT HEAT FLUXES

The estimation of atmospheric turbulent fluxes (or evaporation when the latent heat flux is expressed in water depth;

in this article, evaporation refers to the rate of the conversion of liquid water to water vapor from water, soil surfaces, and through vegetation) at the land surface has long been recognized as the most important process in the determination of the exchanges of energy and mass among hydrosphere, atmosphere, and biosphere (e.g. Bowen, 1926; Penman, 1948; Monteith, 1965; Priestley and Taylor, 1972; Brutsaert, 1982; Morton, 1983; Menenti, 1984; Famiglietti and Wood, 1994; Sellers *et al.*, 1996; Su and Menenti, 1999). Conventional techniques that employ point measurements to estimate the components of energy balance are only representative of local scales and cannot be extended to large areas because of the heterogeneity of the land surface and the dynamic nature of heat transfer processes. Remote sensing is probably the only technique that can provide representative measurements of several relevant physical parameters at scales from a point to the whole globe (Su and Jacobs, 2001). Techniques using remote sensing information to estimate atmospheric turbulent fluxes are therefore essential when dealing with processes that cannot be represented only by point measurements.

In developing remote sensing algorithms for the estimation of atmospheric turbulent fluxes, two basic physical principles, the conservation of energy and turbulent transport, must be considered. The former is the basis of the energy balance approach, and the major challenge is the ability to determine the various physical quantities involved with the required accuracy. The rationale behind the energy balance approach is that evaporation is a change of state of water by demanding a supply of energy for vaporization. The whole problem then reduces to determine all other sources and sinks for energy such as to leave evaporation as the only unknown. The latter recognizes the importance of wind in transporting vapor away from the evaporating surface and, when successful, providing a direct estimate to evaporation. This is often called the *aerodynamic approach* and employs, typically, gradients of wind velocity, temperature, and water vapor density in the near-surface atmosphere where the measurements of these gradients are available. Since the energy budget (i.e., available energy to the surface less the soil heat flux) in the energy balance approach needs to be distributed between sensible heat and latent heat fluxes, which involves, again, the principle of turbulent transport, a complete treatment of both the conservation of energy and turbulent transport processes becomes necessary for developing relevant remote sensing algorithms for these fluxes.

In general, we can distinguish two types of methodologies in remote sensing of turbulent heat fluxes and evaporation: analytical versus (semi-) empirical. The former takes into consideration detailed physical processes at the scale of interest but usually involves complex relationships and requires various input variables, including those that can be observed directly by radiometric measurements

and meteorological variables at a proper reference height. The latter tries to employ empirical relationships and data available chiefly from remote sensing observations. Representative works of the first type include, among others, Jackson *et al.* (1981, 1988) that derived the Crop Water Stress Index (CWSI) by applying the Penman–Monteith equation (Monteith, 1981) to radiometric measurements; Kalma and Jupp (1990), who utilized the dual-source model proposed by Shuttleworth and Wallace (1985), which, by itself, was an extension of the Penman–Monteith approach to take into account the soil and the canopy explicitly; Moran *et al.* (1994) further extended the CWSI approach to partial canopies (the so-called trapezoid-method). More recent work in the same line are those of Chehbouni *et al.* (2001) and Boegh *et al.* (2002), who thoroughly examined the CWSI concept for its strengths and weakness using detailed field measurements collected in Denmark. Other relevant works but of different concepts are those of Chanzy *et al.* (1995) for soil evaporation and Norman *et al.* (1995) using a new type of dual-source model aiming at utilizing directional radiometric measurements. More recently, Kustas and Norman (1999) applied actual soil and vegetation component temperatures to the dual-source model of Norman *et al.* (1995) but did not obtain better results than using only composite temperature without changing the applied Priestley and Taylor (1972) coefficient to a much high value. Mecikalski *et al.* (1999) have applied the Norman *et al.* (1995) approach to continental scale with encouraging results. Efforts related to combined modeling and data assimilation using radiometric measurements have been reported by Castelli *et al.* (1999), Olioso *et al.* (2002), Boni *et al.* (2001a, b), and Caparrini *et al.* (2003, 2004).

Where the (semi) empirical approaches are concerned, the earlier works of Jackson *et al.* (1977) and Seguin and Itier (1983) are representative and many more recent works still follow the same type of approaches but incorporate more remote sensing variables (e.g. in Nishida *et al.*, 2003a, b, besides using remotely sensed surface radiometric temperature as in Jackson *et al.* (1977), vegetation index is also used).

In addition, Menenti (1993), Carlson *et al.* (1995), Kustas and Norman (1996), and Zhang (1996) have provided excellent reviews to the then up-to-date approaches in remote sensing of turbulent heat fluxes and evaporation.

Similarly, the progress made in Wageningen, the Netherlands, can also be mapped in the analytical *versus* (semi-) empirical fashion. The foundation of the analytical approaches were laid by Menenti (1984) by proposing a two-layer combination equation for a drying soil that was later shown by Menenti (1993) to be able to reduce to the Penman–Monteith combination equation and was also shown by Stanghellini (1987) to be equally valid for a green-house canopy. In a further attempt, Menenti and Choudhury (1993) extended the CWSI concept to the

so-called Surface Energy Balance Index (SEBI) approach. While the CWSI was based on surface meteorological scaling, the SEBI concept used Planetary Boundary Layer (PBL) Scaling. However, the parameterization used in SEBI was limited to the then state-of-the-art concepts, namely, the ratio between aerodynamic roughness and thermal dynamic roughness was taken as 10 and the stratification correction was simply taken as 2.9. Application of the SEBI concept to the Aral Sea by Menenti *et al.* (2001) revealed that the parameterization was probably not universal and caused some unexplained scatters in the results. More recently, Su (2002) has proposed the Surface Energy Balance System (SEBS) by extending the SEBI concept with a dynamic model for thermal roughness (Su *et al.*, 2001), the Bulk Atmospheric Similarity (BAS) theory of Brutsaert (1999) for PBL scaling, and the Monin–Obukhov Atmospheric Surface Layer (ASL) similarity for surface layer scaling such that SEBS can be used for both local scaling and regional scaling under all atmospheric stability regimes, thus providing a link for radiometric measurements and atmospheric models at various scales. Using SEBS, Jia *et al.* (2003) have successfully coupled model forecast fields of a large scale Numerical Weather Prediction (NWP) model to radiometric measurements from the Along Track Scanning Radiometer (ATSR) onboard the European Remote Sensing Satellite (ERS-2). Rauwerda *et al.* (2002) have extended SEBS to a parallel-source model and have showed significant improvement in estimated turbulent heat fluxes. On the application side, SEBS has been used to generate daily, monthly, and annual evaporation in a semiarid environment (Li, 2001; Su *et al.*, 2003a) and for drought monitoring (Su *et al.*, 2003b). Another development is that of Jia *et al.* (2001), who have proposed a dual-source model for using component (soil and vegetation) temperatures such as those derivable from ATSR data. The scheme is similar to the Shuttleworth and Wallace (1985) dual-source model but employs the boundary-resistance formulation of Stanghellini (1987) and shows much flexibility in dealing with heterogeneous surfaces.

On the empirical side, the work of Nieuwenhuis *et al.* (1985) was among the earliest attempts but was valid only for single crops. Later, Bastiaanssen (1995) proposed the Surface Energy Balance Algorithm for Land (SEBAL) that required simultaneous presence of absolute dry and wet pixels and has been used for many irrigation studies. More recently, Su *et al.* (1999) have made correction in SEBAL to remedy a theoretical problem and added a scheme to apply NWP fields with an up-scaling and down-scaling approach. In another effort, Roerink *et al.* (2000) proposed a Simplified Surface Energy Balance Index (S-SEBI) by fitting dry and wet cases present in the spatial radiometric data and showed reasonable success for application to semiarid areas.

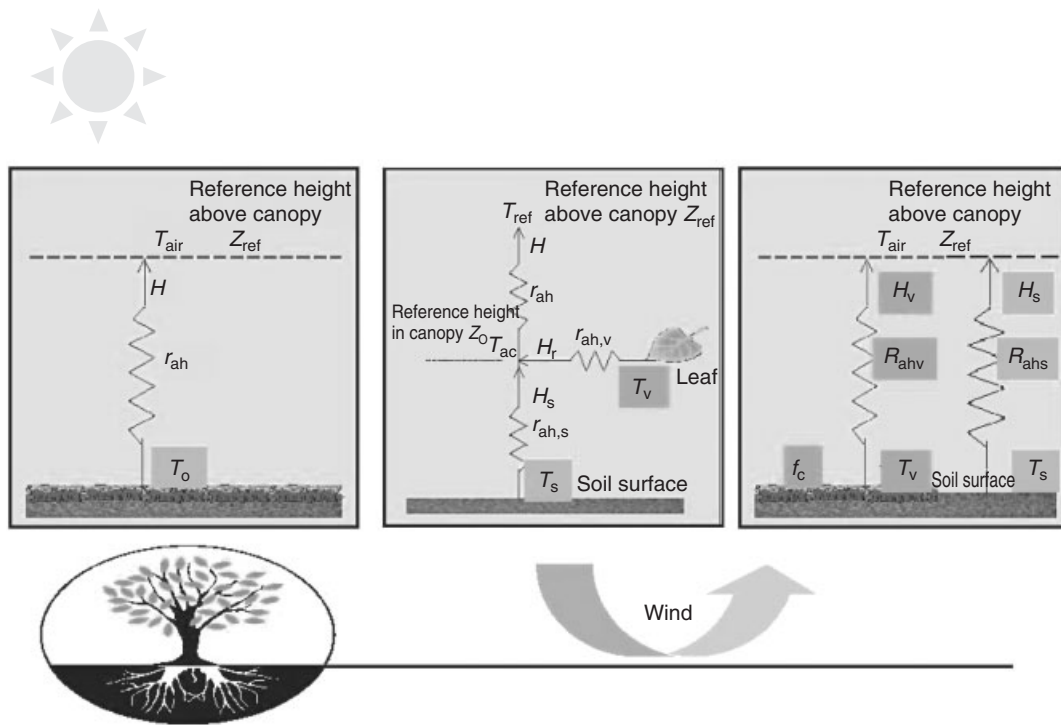


**Figure 1** Flux parameterization schemes. Remote sensing of heat fluxes and evaporation – single-source, dual-source, and parallel-source has been shown in the figure. A color version of this image is available at <http://www.mrw.interscience.wiley.com/ehs>

In order to give a clear picture of the differences in various schemes encountered in turbulent heat fluxes parameterization, Figure 1 summarizes the single-source, dual-source, and parallel-source schemes. In the following, we will review the difficulties and the relationships between radiometric measurements and atmospheric boundary meteorological variables in estimation of turbulent heat fluxes by means of SEBS (Su, 2002).

### THE SURFACE ENERGY BALANCE SYSTEM (SEBS) FOR ESTIMATION OF TURBULENT HEAT FLUXES AND EVAPORATION

SEBS was developed for the estimation of atmospheric turbulent fluxes using satellite earth observation data more coherently. SEBS, as proposed by Su (2002), consists of: a set of tools for the determination of the land surface physical parameters, such as albedo, emissivity, temperature, vegetation coverage, and so on, from spectral reflectance and radiance; an extended model for the determination of the roughness length for heat transfer of Su *et al.* (2001); and a new formulation for the determination of the evaporative fraction on the basis of energy balance at limiting cases. In the application, SEBS requires as inputs three sets of information. The first set consists of land surface

albedo, emissivity, temperature, fractional vegetation coverage and leaf area index, and the height of the vegetation (or roughness height). When vegetation information is not explicitly available, the Normalized Difference Vegetation Index (NDVI) is used as a surrogate. These inputs can be derived from remote sensing data in conjunction with other information about the concerned surface. The second set includes air pressure, temperature, humidity, and wind speed at a reference height. The reference height is the measurement height for point application and the height of the PBL for regional application (in this latter case, PBL-averaged meteorological variables are to be used. See later for detailed discussions). This data set can also be variables estimated by a large-scale meteorological model. The third data set includes downward solar radiation and downward longwave radiation that can either be direct measurements, model output, or parameterization.

In SEBS, the friction velocity, the sensible heat flux, and the Obukhov stability length are obtained by solving the system of nonlinear equations. For field measurements performed at a height of a few meters above ground, since the surface fluxes are related to surface variables and variables in the atmospheric surface layer, all calculations use the Monin–Obukhov Similarity (MOS) functions given by Brutsaert (1999). By replacing the MOS stability functions with the Bulk Atmospheric Boundary Layer

Similarity (BAS) functions proposed by Brutsaert (1999), the system equations can be used to relate surface fluxes to surface variables and the mixed layer atmospheric variables provided either by radiosonde data or obtained from atmospheric model fields. The relevant atmospheric boundary layer (ABL) that needs to be considered in different scaling is shown in Figure 2 (*see also Chapter 29, Atmospheric Boundary-Layer Climates and Interactions with the Land Surface, Volume 1*). The determination of the evaporative fraction (the ratio of latent heat flux to the available energy) on the basis of energy balance at limiting cases is carried out, and, finally, the turbulent heat fluxes are determined by utilizing the surface energy balance. Further, by utilizing the conservative characteristics of the evaporative fraction, the daily evaporation can be determined, given the total daily available energy. The different steps involved in SEBS are discussed below.

### Determination of Evaporative Fraction Based On Energy Balance at Limiting Cases

The surface energy balance is written in SEBS as

$$R_n = G_0 + H + \lambda E \quad (1)$$

where  $R_n$  is the net radiation,  $G_0$  is the soil heat flux,  $H$  is the turbulent sensible heat flux, and  $\lambda E$  is the turbulent latent heat flux ( $\lambda$  is the latent heat of vaporization and  $E$  is the actual evapotranspiration).

The equation to calculate the net radiation is given by

$$R_n = (1 - \alpha) \cdot R_{swd} + \varepsilon \cdot R_{lwd} - \varepsilon \cdot \sigma \cdot T_0^4 \quad (2)$$

where  $\alpha$  is the albedo,  $R_{swd}$  is the downward solar radiation,  $R_{lwd}$  is the downward longwave radiation,  $\varepsilon$  is the emissivity of the surface,  $\sigma$  is the Stefan-Boltzmann constant, and  $T_0$  is the surface radiative temperature measured by a remote sensor (*see also Chapter 52, Estimation of Surface Temperature and Surface Emissivity, Volume 2*).  $\alpha$ ,  $\varepsilon$ , and  $T_0$  can be derived from remote sensing data from the visible to the thermal infrared spectral range. The simplest of form to calculate the downward solar radiation is  $R_{swd} = I_{sc} \cdot e_0 \cdot \cos \theta_z \cdot \exp(-m \cdot \tau)$ , where  $I_{sc} = 1367 \text{ W} \cdot \text{m}^{-2}$  is the solar constant,  $e_0$  the eccentricity factor,  $\theta_z$  the solar zenith angle,  $m$  the air mass, and  $\tau$  the optical thickness. Details on the determination of all the parameters can be found in Iqbal (1983) (*see also Chapter 39, Surface*

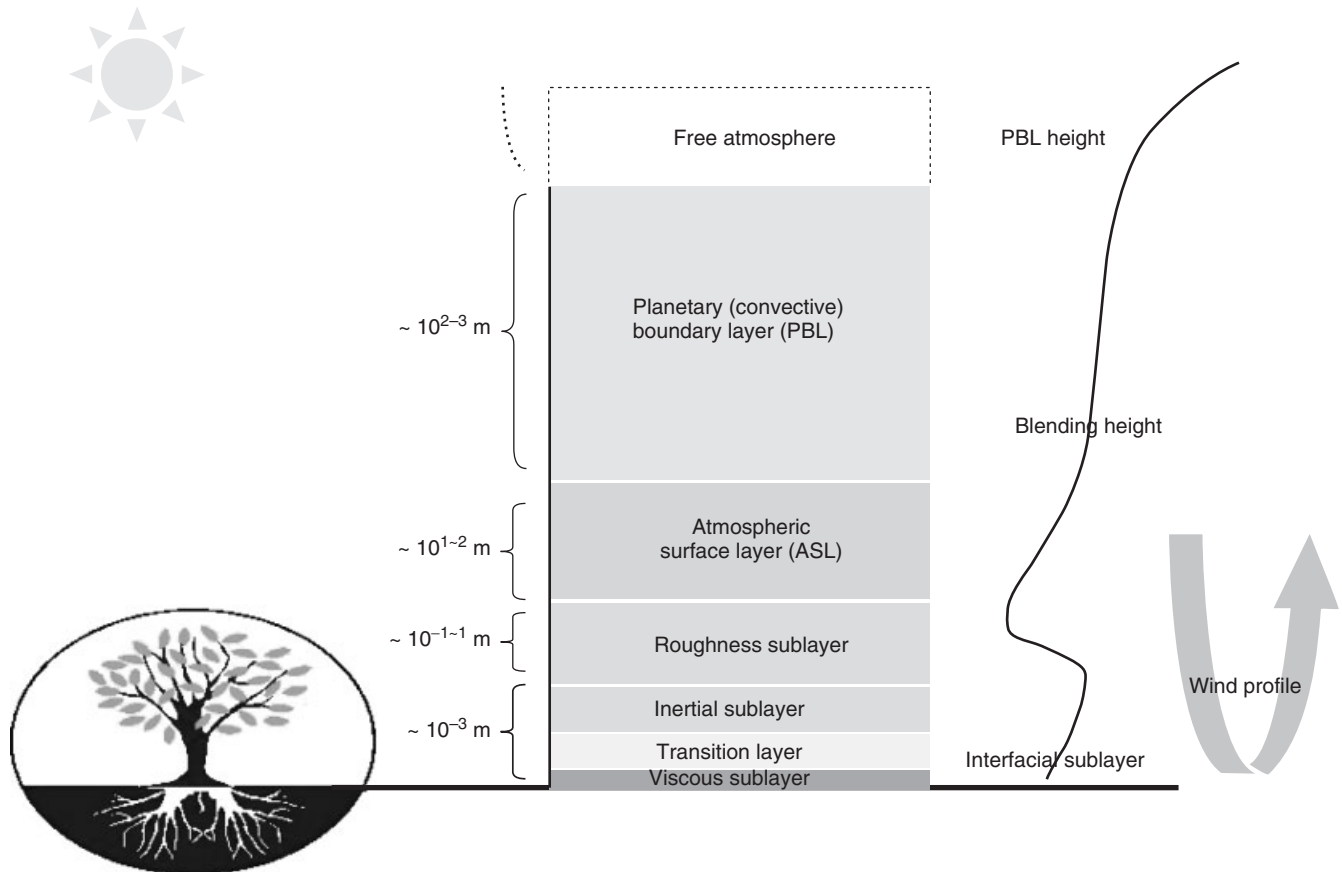


**Figure 2** Typical structure of the atmospheric boundary layer. SEBS includes both surface scaling and PBL scaling. A color version of this image is available at <http://www.mrw.interscience.wiley.com/ehs>

**Radiation Balance, Volume 1).** The downward longwave radiation  $R_{lwd}$  can be calculated as  $R_{lwd} = \varepsilon_a \sigma T_a^4$  when there is no measurement, where  $\varepsilon_a$  is the emissivity of the atmosphere that can be estimated using the Swinbank formula as given by Campbell and Norman (1998) in the form  $\varepsilon_a = 9.2 \cdot 10^{-6} \cdot (T_a + 273.15)^2$ , with  $T_a$  the air temperature at the reference height. Su *et al.* (2001) and Su (2002) have shown that equation (2) provides accurate estimation of the net radiation.

The equation to calculate the soil heat flux is parameterized as

$$G_0 = R_n \cdot [\Gamma_c + (1 - f_c) \cdot (\Gamma_s - \Gamma_c)] \quad (3)$$

in which it is assumed that the ratio of soil heat flux to net radiation is  $\Gamma_c = 0.05$  for full vegetation canopy (Monteith, 1973) and  $\Gamma_s = 0.315$  for bare soil (Kustas and Daughtry, 1989). An interpolation is then performed between these limiting cases using the fractional canopy coverage,  $f_c$ , which can be determined from remote sensing data.

In order to determine the evaporative fraction, energy balance considerations at limiting cases are used. Under the dry limit, the latent heat (or the evaporation) becomes zero due to the limitation of soil moisture, and the sensible heat flux is at its maximum value. From equation (1), it follows,

$$\begin{aligned} \lambda E_{\text{dry}} &= R_n - G_0 - H_{\text{dry}} \equiv 0, \\ \text{or } H_{\text{dry}} &= R_n - G_0 \end{aligned} \quad (4)$$

Under the wet limit, where the evaporation takes place at potential rate,  $\lambda E_{\text{wet}}$ , (i.e., the evaporation is only limited by the available energy under the given surface and atmospheric conditions), the sensible heat flux takes its minimum value,  $H_{\text{wet}}$ , that is,

$$\begin{aligned} \lambda E_{\text{wet}} &= R_n - G_0 - H_{\text{wet}}, \\ \text{or } H_{\text{wet}} &= R_n - G_0 - \lambda E_{\text{wet}} \end{aligned} \quad (5)$$

The relative evaporation then can be evaluated as

$$\Lambda_r = \frac{\lambda E}{\lambda E_{\text{wet}}} = 1 - \frac{\lambda E_{\text{wet}} - \lambda E}{\lambda E_{\text{wet}}} \quad (6)$$

By substituting equations (1), (5), and (4) in equation (6) and after some algebra, one obtains

$$\Lambda_r = 1 - \frac{H - H_{\text{wet}}}{H_{\text{dry}} - H_{\text{wet}}} \quad (7)$$

The evaporative fraction is finally given by:

$$\Lambda = \frac{\lambda E}{H + \lambda E} = \frac{\lambda E}{R_n - G} = \frac{\Lambda_r \cdot \lambda E_{\text{wet}}}{R_n - G} \quad (8)$$

Equations (1–8) constitute the basis formulation of SEBS. Further, in SEBS, the actual sensible heat flux  $H$  is obtained by solving a set of non-linear equations and is constrained in the range set by the sensible heat flux at the wet limit  $H_{\text{wet}}$ , and the sensible heat flux at the dry limit  $H_{\text{dry}}$ .

### Determination of Sensible Heat Fluxes $H$ , $H_{\text{dry}}$ , $H_{\text{wet}}$

In order to derive the actual sensible heat flux  $H$ , the similarity theory is used. In SEBS, distinction is made between the ABL or PBL and the Atmospheric Surface Layer (ASL) similarity. ABL refers to the part of atmosphere that is directly influenced by the presence of the Earth's surface and responds to the surface forcings with a timescale of an hour or less, while ASL refers to usually the bottom 10% of ABL but above the roughness sublayer, that is, the ASL is where turbulent fluxes and stress vary by less than 10% of their magnitude (Stull, 1988; *see also Chapter 29, Atmospheric Boundary-Layer Climates and Interactions with the Land Surface, Volume 1*). The roughness sublayer (or the interfacial layer) is the near-surface thin layer of a few centimeters where the molecular transport dominates over turbulent transport (see Figure 2). The thickness of the roughness sublayer is thought to be around 35 times the surface roughness height, or three times the vegetation height (Katul and Parlange, 1992). In ASL, the similarity relationships for the profiles of the mean wind speed,  $u$ , and the mean temperature,  $\theta_0 - \theta_a$ , can be written in integral form as

$$u = \frac{u_*}{k} \left[ \ln \left( \frac{z - d_0}{z_{0m}} \right) - \Psi_m \left( \frac{z - d_0}{L} \right) + \Psi_m \left( \frac{z_{0m}}{L} \right) \right] \quad (9)$$

$$\begin{aligned} \theta_0 - \theta_a &= \frac{H}{k u_* \rho C_p} \left[ \ln \left( \frac{z - d_0}{z_{0h}} \right) - \Psi_h \left( \frac{z - d_0}{L} \right) \right. \\ &\quad \left. + \Psi_h \left( \frac{z_{0h}}{L} \right) \right] \end{aligned} \quad (10)$$

where  $z$  is the height above the surface,  $u_* = (\tau_0/\rho)^{1/2}$  is the friction velocity,  $\tau_0$  is the surface shear stress,  $\rho$  is the density of air,  $k = 0.4$  is the von Karman constant,  $d_0$  is the zero-plane displacement height,  $z_{0m}$  is the roughness height for momentum transfer,  $\theta_0$  is the potential temperature at the surface,  $\theta_a$  is the potential air temperature at height  $z$ ,  $z_{0h}$  is the scalar roughness height for heat transfer,  $\Psi_m$  and  $\Psi_h$  are the stability correction functions for momentum and sensible heat transfer respectively,  $L$  is the Obukhov length defined as

$$L = -\frac{\rho C_p u_*^3 \theta_v}{k g H} \quad (11)$$

where  $g$  is the acceleration due to gravity,  $\theta_v$  is the potential virtual temperature near the surface.

For field measurements performed at a height of a few meters above ground, clearly, since the surface fluxes are related to surface variables and variables in the atmospheric surface layer, all calculations use the MOS stability functions (e.g. Brutsaert, 1999). By replacing the MOS stability functions with the BAS functions proposed by Brutsaert (1999), the system of equations (9–11) can be used to relate surface fluxes to surface variables and the mixed layer atmospheric variables. The criterion proposed by Brutsaert (1999) is used to determine if the MOS or the BAS scaling is appropriate for a given situation. The above functions are valid for unstable conditions only. For stable conditions, the expressions proposed by Beljaars and Holtslag (1991) and evaluated by Van den Hurk and Holtslag (1995) are used for atmospheric surface layer scaling, and the functions proposed by Brutsaert (1982, p. 84) for ABL scaling.

The friction velocity, the sensible heat flux, and the Obukhov stability length are obtained by solving the system of nonlinear equations (9–11) using the method of Broyden (Press *et al.*, 1997). It is important to note that the derivation of the sensible heat flux using equations (9–11) requires only the wind speed and temperature at the reference height as well as the surface temperature, and is independent of other surface energy balance terms.

As stated previously, this derived actual sensible heat flux  $H$  is further subjected to constraints in the range set by the sensible heat flux at the wet limit  $H_{\text{wet}}$ , and the sensible heat flux at the dry limit  $H_{\text{dry}}$  in SEBS.

The sensible heat flux at the dry limit  $H_{\text{dry}}$  is given by equation (4) and the sensible heat flux at the wet limit  $H_{\text{wet}}$  can be derived by combining equation (5) and a combination equation similar to the Penman–Monteith combination equation (Monteith, 1965). Menenti (1984) showed, when the resistance terms are grouped into the bulk internal (or surface) and external (or aerodynamic) resistances, the combination equation can be written in the following form,

$$\lambda E = \frac{\Delta \cdot r_e \cdot (R_n - G_0) + \rho C_p \cdot (e_{\text{sat}} - e)}{r_e \cdot (\gamma + \Delta) + \gamma \cdot r_i} \quad (12)$$

where  $e$  and  $e_{\text{sat}}$  are actual and saturation vapor pressure, respectively;  $\gamma$  is the psychrometric constant, and  $\Delta$  is the rate of change of saturation vapor pressure with temperature (i.e.  $\partial e_{\text{sat}}(T)/\partial T$ );  $r_i$  is the bulk surface internal resistance, and  $r_e$  is the external or aerodynamic resistance. In the above equation, it is assumed that the roughness lengths for heat and vapor transfer are the same (Brutsaert, 1982). It is worthwhile to point out that the Penman–Monteith equation is strictly only valid for vegetation canopy, whereas the definition by means of equation (12) is also valid for soil surface with properly defined bulk internal resistance. The difficulty in using equation (12) to estimate latent heat flux

lies in the difficulty to determine the bulk internal resistance  $r_i$ , which is strongly regulated by soil water availability. Because the latter is generally not known *a priori*, an alternative is thus proposed in SEBS to avoid the direct use of  $r_i$  in estimating  $\lambda E$ .

At the wet limit, the internal resistance  $r_i \equiv 0$  by definition. Using this property in equation (12) and changing the subscripts correspondingly to reflect the wet-limit condition, the sensible heat flux at the wet limit is obtained as

$$H_{\text{wet}} = \left( (R_n - G_0) - \frac{\rho C_p}{r_{ew}} \cdot \frac{e_s - e}{\gamma} \right) / \left( 1 + \frac{\Delta}{\gamma} \right) \quad (13)$$

The external resistance depends also on the Obukhov length,  $L$ , which in turn is a function of the friction velocity and sensible heat flux (equation 11). With the friction velocity and the Obukhov length determined by the numerical procedure described previously, the external resistance can be determined from equation (10) as

$$r_e = \frac{1}{ku_*} \left[ \ln \left( \frac{z - d_0}{z_{0h}} \right) - \Psi_h \left( \frac{z - d_0}{L} \right) + \Psi_h \left( \frac{z_{0h}}{L} \right) \right] \quad (14)$$

Similarly, the external resistance at the wet limit can be derived as

$$r_{ew} = \frac{1}{ku_*} \left[ \ln \left( \frac{z - d_0}{z_{0h}} \right) - \Psi_h \left( \frac{z - d_0}{L_w} \right) + \Psi_h \left( \frac{z_{0h}}{L_w} \right) \right] \quad (15)$$

and the wet-limit stability length can be determined as

$$L_w = - \frac{\rho u_*^3}{kg \cdot 0.61 \cdot (R_n - G_0) / \lambda} \quad (16)$$

### Determination of the Roughness Length for Heat Transfer

In the above derivations, the aerodynamic and thermal dynamic roughness parameters need to be known first. When near-surface wind speed and vegetation parameters (height and leaf area index) are available, the within-canopy turbulence model proposed by Massman (1997) can be used to estimate aerodynamic parameters,  $d_0$ , the displacement height, and  $z_{0m}$ , the roughness height for momentum. This model has been shown by Su *et al.* (2001) to produce reliable estimates of the aerodynamic parameters. If only the height of the vegetation is available, the relationships proposed by Brutsaert (1982) can be used. If a detailed land-use classification is available, the tabulated values of Wieringa (1993) can be used. However, since the aerodynamic parameters depend also on wind speed and wind direction besides the surface characteristics, the latter two approaches should only be used when the first method

cannot be used due to lack of data. When all of the above information is not available or not convenient to use, the aerodynamic parameters can be related to vegetation indices derived from satellite data. However, in this case, care must be taken, because the vegetation indices saturate at higher vegetation densities and the relationships are vegetation-type dependent.

The scalar roughness height for heat transfer,  $z_{0h}$ , changes with surface characteristics, atmospheric flow, and thermal dynamic state of the surface (Blümel, 1999; Massman, 1999a). Based on the work of Massman (1999a), a simple roughness model for heat transfer was proposed by Su *et al.* (2001). However, in their model, a functional form to describe the vertical structure of the vegetation canopy is needed in order to calculate the within-canopy wind speed profile extinction coefficient,  $n_{ec}$ . For local studies, this information is easily obtained, but for large-scale applications, it is generally impossible to obtain detailed information on the vertical structure of the canopy. In SEBS,  $n_{ec}$ , is formulated as a function of the cumulative leaf drag area at the canopy top,

$$n_{ec} = \frac{C_d \cdot LAI}{2u_*^2/u(h)^2} \quad (17)$$

where  $C_d$  is the drag coefficient of the foliage elements assumed to take the value of 0.2,  $LAI$  is the one-sided leaf area index defined for the total ground area, and  $u(h)$  is the horizontal wind speed at the canopy top. The scalar roughness height for heat transfer,  $z_{0h}$ , can be derived from

$$z_{0h} = \frac{z_{0m}}{\exp(kB^{-1})} \quad (18)$$

where  $B^{-1}$  is the inverse Stanton number, a dimensionless heat transfer coefficient. To estimate the  $kB^{-1}$  value, an extended model of Su *et al.* (2001) is proposed as follows,

$$kB^{-1} = \frac{kC_d}{4C_t \frac{u_*}{u(h)} (1 - e^{-n_{ec}/2})} f_c^2 + 2f_c f_s \frac{k \cdot u_*/u(h) \cdot z_{0m}/h}{C_t^*} + kB_s^{-1} f_s^2 \quad (19)$$

where  $f_c$  is the fractional canopy coverage and  $f_s$  is its complement.  $C_t$  is the heat transfer coefficient of the leaf. For most canopies and environmental conditions,  $C_t$  is bounded as  $0.005N \leq sC_t \leq 0.075N$  ( $N$  is number of sides of a leaf to participate in heat exchange). The heat transfer coefficient of the soil is given by  $C_t^* = Pr^{-2/3} Re_*^{-1/2}$ , where  $Pr$  is the Prandtl number, the roughness Reynolds number  $Re_* = h_s u_*/\nu$ , with  $h_s$  the roughness height of the soil. The kinematic viscosity of the air is given by  $\nu = 1.327 \cdot 10^{-5} (p_0/p) (T_a/T_{a0})^{1.81}$  (Massman, 1999b), with  $p$  and  $T_a$

the ambient pressure and temperature, and  $p_0 = 101.3 \text{ kPa}$  and  $T_{a0} = 273.15 \text{ K}$ . Physically and geometrically, the first term of equation (19) follows the full canopy-only model of Choudhury and Monteith (1988), the third term is that of Brutsaert (1982) for a bare soil surface, while the second term describes the interaction between vegetation and bare soil surface. A quadratic weighting based on the fractional canopy coverage is used to accommodate any situation between the full vegetation and bare soil conditions. For bare soil surface,  $kB_s^{-1}$  is calculated according to Brutsaert (1982)

$$kB_s^{-1} = 2.46(Re_*)^{1/4} - \ln[7.4] \quad (20)$$

### The MOS Stability Correction Functions

The MOS stability correction functions for momentum and sensible heat transfer  $\psi_m$  and  $\psi_h$ , respectively, are defined in the following integrated form

$$\Psi_i(y) = \int_0^y [1 - \phi_i(x)] \frac{dx}{x} \quad (21)$$

where  $y = -(z - d)/L \cdot i$  equals  $m$ , or  $h$  for momentum and sensible heat transfer, respectively.

The  $\phi_i$  functions are proposed by Brutsaert (1999) as

$$\phi_m(y) = \frac{\left(a + b \cdot y^{m+1/3}\right)}{a + y^m} \quad (22)$$

$$\phi_h(y) = \frac{(c + d \cdot y^n)}{c + y^n} \quad (23)$$

On the basis of data reported by Högström (1988) and Kader and Yaglom (1990), Brutsaert (1999) assigned the constants in equations (22–23) as  $a = 0.33$ ,  $b = 0.41$ ,  $m = 1.0$ ,  $c = 0.33$ ,  $d = 0.057$ , and  $n = 0.78$ .

Upon integration of equations (22) and (23) using equation (21), the required MOS stability functions for free convective conditions are obtained.

$$\begin{aligned} \Psi_m(y) = & \ln(a + y) - 3 \cdot b \cdot y^{1/3} \\ & + \frac{b \cdot a^{1/3}}{2} \ln \left[ \frac{(1 + x)^2}{(1 - x + x^2)} \right] \\ & + 3^{1/2} \cdot b \cdot a^{1/3} \tan^{-1} \left[ \frac{(2 \cdot x - 1)}{3^{1/2}} \right] \\ & + \Psi_0, \quad \text{for } y \leq b^{-3} \end{aligned} \quad (24a)$$

$$\Psi_m(y) = \Psi_m(b^{-3}), \quad \text{for } y > b^{-3} \quad (24b)$$

$$\Psi_h(y) = \left[ \frac{(1 - d)}{n} \right] \ln \left[ \frac{(c + y^n)}{c} \right] \quad (25)$$

where  $x = (y/a)^{1/3} \cdot \Psi_0 = (-\ln a + 3^{1/2} \cdot b \cdot a^{1/3} \cdot \pi/6)$  is an integration constant.

Equations (24–25) are extensions to the Businger–Dyer function for unstable conditions. For stable conditions, the expressions proposed by Beljaars and Holtslag (1991) and evaluated by Van den Hurk and Holtslag (1995) can be used. These are given below:

$$\Psi_m(y_s) = - \left[ a_s \cdot y_s + b_s \left( y_s - \frac{c_s}{d_s} \right) \cdot \exp(-d_s \cdot y_s) + \frac{b_s \cdot c_s}{d_s} \right] \quad (26)$$

$$\Psi_h(y_s) = - \left[ \left( 1 + \frac{2a_s}{3} y_s \right)^{1.5} + b_s \cdot \left( y_s - \frac{c_s}{d_s} \right) \cdot \exp(-d_s \cdot y_s) + \left( \frac{b_s \cdot c_s}{d_s} - 1 \right) \right] \quad (27)$$

where  $y_s = (z - d)/L$ ,  $a_s = 1$ ,  $b_s = 0.667$ ,  $c_s = 5$  and  $d_s = 1$ .

### The Bulk Atmospheric Boundary Layer (ABL) Similarity (BAS) Stability Correction Functions

Under free convective conditions, the outer region of the ABL is well mixed such that the mean profiles of wind and potential temperature are nearly constant with height. This is equivalent to state that the unstable ABL consists of two regions, an inner region where MOS is valid, and a slab outer region where the profiles are constant.

According to Brutsaert (1999), experimental evidence suggests that the height of the ASL,  $h_{st}$ , should be scaled with the thickness of the ABL over moderately rough surfaces, but with the surface roughness over very rough terrain. More quantitatively,  $h_{st}$ , can be determined in the following ways

$$h_{st} = \alpha_b \cdot h_i \quad (28)$$

where  $h_i$  is the height of the ABL and  $\alpha_b$  is around 0.10–0.15, or

$$h_{st} = \beta_b \cdot z_0 \quad (29)$$

where  $\beta_b$  is around 100–150 whichever is larger. Setting typical values of  $\beta_b/\alpha_b = 10^3$ , and  $h_i = 10^3$  m, gives  $z_0 = (\alpha_b/\beta_b) \cdot h_i = 1$  m, which separates very rough from moderate rough terrain.

For moderately rough terrain satisfying  $z_0 < (\alpha_b/\beta_b) \cdot h_i$ , joining the inner with the outer region such that  $u(z - d_0) = u_m$ ,  $\theta_a(z - d_0) = \theta_m$ , at  $z - d_0 = h_{st}$ , (where the subscript  $m$  indicates average of the variable in question over the lower half of the mixed layer, which is an advise for practical applications because the entrainment of warmer air into the ABL affects both the potential

temperature and the wind profiles in the upper half of the ABL), allows to derive the bulk stability functions

$$B_w = -\ln(\alpha_b) + \Psi_m \left( \frac{\alpha_b \cdot h_i}{L} \right) - \Psi_m \left( \frac{z_0}{L} \right) \quad (30)$$

$$C_w = -\ln(\alpha_b) + \Psi_h \left( \frac{\alpha_b \cdot h_i}{L} \right) - \Psi_h \left( \frac{z_0}{L} \right) \quad (31)$$

Equations (30–31) show that the bulk stability functions depend on both the surface roughness and the height of the ABL for moderately rough terrain.

Similarly, for very rough terrain, that is,  $z_0 \geq (\alpha_b/\beta_b) \cdot h_i$ , we obtain

$$B_w = -\ln \left( \frac{h_i}{(\beta_b \cdot z_0)} \right) + \Psi_m \left( \frac{\beta_b \cdot z_0}{L} \right) - \Psi_m \left( \frac{z_0}{L} \right) \quad (32)$$

$$C_w = -\ln \left( \frac{h_i}{(\beta_b \cdot z_0)} \right) + \Psi_h \left( \frac{\beta_b \cdot z_0}{L} \right) - \Psi_h \left( \frac{z_0}{L} \right) \quad (33)$$

which state that the bulk stability functions depend on only the surface roughness for very rough terrain.

Finally, for stable conditions, that is, when  $h_i/L > 0$ , we use (Brutsaert, 1982, equation 4.93, p. 84)

$$B_w = -2.2 \cdot \ln \left( 1 + \frac{h_i}{L} \right) \quad (34)$$

$$C_w = -7.6 \cdot \ln \left( 1 + \frac{h_i}{L} \right) \quad (35)$$

Both stability correction functions may need to be verified using data from more recent large-scale field experiment and updated accordingly when necessary.

### Determination of Turbulent Heat Fluxes and Actual Evaporation

By inverting equation (8), the actual sensible and latent heat fluxes can be obtained as,

$$H = (1 - \Lambda) \cdot (R_n - G) \\ \lambda E = \Lambda \cdot (R_n - G) \quad (36)$$

When the evaporative fraction is known, the daily evaporation can be determined as

$$E_{\text{daily}} = 8.64 \times 10^7 \times \int_0^{24} \times \frac{\overline{R_n} - \overline{G_0}}{\lambda \rho_w} \quad (37)$$

where  $E_{\text{daily}}$  is the actual evaporation on daily basis ( $mm \cdot d^{-1}$ )  $\cdot \int_0^{24}$  is the daily average evaporative fraction, which can be approximated by the SEBS estimate since

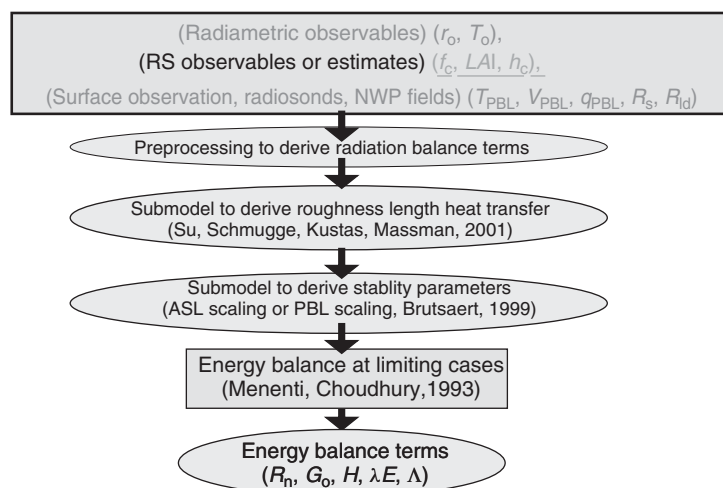


**Figure 3** Schematic representation of SEBS. A color version of this image is available at <http://www.mrw.interscience.wiley.com/ehs>

the evaporative fraction is conservative (Shuttleworth *et al.*, 1989; Sugita and Brutsaert, 1991; Crago, 1996).  $\overline{R}_n$  and  $\overline{G}_o$  are the daily net radiation flux and soil heat flux,  $\lambda$  is the latent heat of vaporization ( $J K g^{-1}$ ),  $\rho_w$  is the density of water ( $K g m^{-1}$ ).

Since the daily soil heat flux is close to zero because the downward flux in daytime and the upward flux at night balance each other approximately, the daily evaporation only depends on the net radiation flux given by

$$\overline{R}_n = (1 - \alpha)K_{24}^\downarrow + \varepsilon L_{24} \quad (38)$$

where  $K_{24}^\downarrow$  is the daily incoming global radiation (*see Chapter 49, Estimation of Surface Insolation, Volume 2*) and  $L_{24}$  is daily net longwave radiation. The daily average albedo,  $\alpha$ , and emissivity,  $\varepsilon$ , can be approximated easily with the same values as used previously in the energy balance equation.

By summing up the corresponding daily evaporation for a certain period, the actual evaporation for that period (i.e., a week, a month, or a year) can be determined. However, errors will occur due to cloud effects. Such effects can be further removed by using the time series processing or by data assimilation procedures. A schematic presentation of SEBS is given in Figure 3 for clarity of the steps involved.

## SOME ISSUES IN THE APPLICATION OF SEBS

### Difficulty in Determination of Aerodynamic Roughness Height

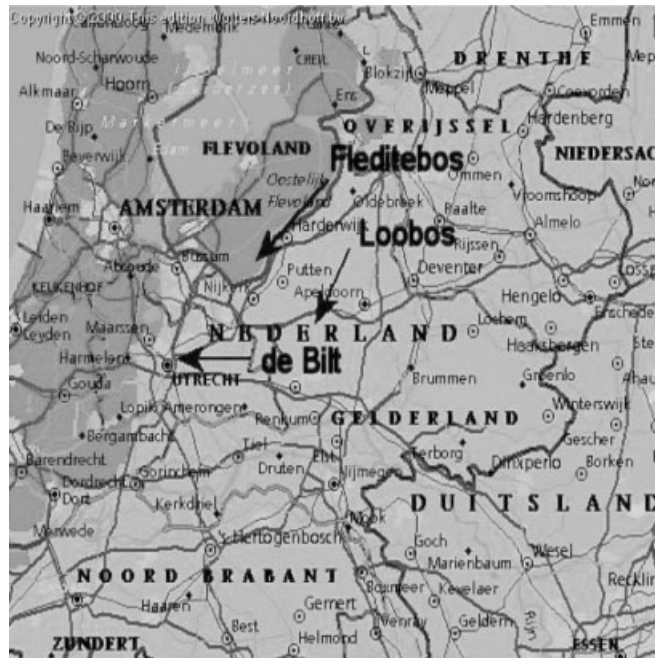
Aerodynamic roughness height (the displacement height is often related to it) influences greatly the turbulent

characteristics near the surface where the heat fluxes originate. Currently, there are several methods that can be used for its determination as shown in Figure 4, including retrievals from wind profiles, which is probably the most accurate method but is limited to the local topographic and canopy structure and varies with wind speed (different fetch) and direction (for heterogeneous terrain). Other methods are based on either vegetation height or land-use

**Table 1** Land-use classes in the PELCOM land-use database and associated  $z_{0m}$  values

	Land-use class	$z_{0m}(m)$
1	Grass	0.0340
2	Maize	0.4966
3	Potatoes	0.0639
4	Beets	0.0639
5	Cereals	0.4966
6	Other crops	0.0639
7	Greenhouses	0.4066
8	Orchards	0.6065
9	Bulbs	0.0639
10	Deciduous forest	1.2214
11	Coniferous forest	1.2214
12	Heather	0.0408
13	Other open spaces in natural areas	0.0408
14	Bare soil in natural areas	0.0012
15	Freshwater	0.0002
16	Salt water	0.0002
17	Continuous urban area	1.1052
18	Built-up area in rural area	0.5488
19	Deciduous forest in urban area	1.2214
20	Coniferous forest in urban area	1.2214
21	Built-up area with dense forest	1.2214
22	Grass in built-up area	0.0334
23	Bare soil in built-up area	0.0012
24	Main roads and railways	0.0035
25	Buildings in rural areas	0.5488

- Retrievals from wind profiles (Point values)
- $z_{0m} = 0.136 * h$  (Vegetation height)
- Land use + look up table ( $z_{0m}$  per class) (e.g. in atmospheric models)
- $z_{0m} \sim$  Vegetation index relationships (e.g.  $z_{0m} = \exp(A+B*NDVI)$ )
- Land use + modelling (Hasager, Jensen, 1999)
- LIDAR measurements (e.g. Menenti, Ritchie, 1994)
- Vegetation canopy LIDAR ???



Measurement sites in the Netherlands

**Figure 4** Summary of some methods used to determine the aerodynamic roughness height. A color version of this image is available at <http://www.mrw.interscience.wiley.com/ehs>

classes, and assigning each class a nominal value, or using a relationship with vegetation index. One particular promising method is that of Hasager and Jensen (1999) that is able to consider the dynamic flow characteristics and actual land-use characteristics. Menenti and Ritchie (1994) showed that airborne LIDAR measurements of vegetation heights provided reliable determination of the aerodynamic roughness, so that a space-borne LIDAR system when available might be quite promising. An example for the aerodynamic roughness height for each classes of the PELCOM land-use map (Pan-European Land-Use and Land-Cover Monitoring, Mùcher *et al.*, 2001) is given in Table 1. Table 2 shows the dependency of the aerodynamic roughness height on wind direction (different land surfaces) and season (summer or winter), and shows the uncertainties that might be encountered when using any of the methods indicated in Figure 4.

At any rate, despite great efforts in the past, the determination of aerodynamic roughness remains a challenging issue for large-scale applications both for remote sensing of surface turbulent heat fluxes and mesoscale and global-scale atmospheric modeling. Figure 5 shows a map of  $z_{0m}$  values for the Netherlands with values corresponding to Table 1.

### Coupling with Large-Scale Numerical Weather Prediction Models

Owing to its flexibility in scaling between surface and atmospheric variables, SEBS can be easily coupled to the meteorological fields generated by a large-scale atmospheric model. A first attempt has been made by Jia *et al.* (2003) to couple model fields from a NWP model to radiometric measurements from the ATSR onboard the European Remote

**Table 2** Effective roughness length (m), representative of a few kilometers of upstream terrain from the Cabauw tower in the Netherlands for 18 wind direction classes (degrees relative to North, after Beljaars and Bosveld, 1997)

Wind direction	0–20	20–40	40–60	60–80	80–100	100–120	120–140	140–160	160–180
Summer	0.06	0.08	0.10	0.15	0.15	0.15	0.11	0.08	0.04
Winter	0.04	0.05	0.05	0.07	0.10	0.12	0.02	0.02	0.02
Wind direction	180–200	200–220	220–240	240–260	260–280	280–300	300–320	320–340	340–360
Summer	0.04	0.04	0.04	0.07	0.06	0.06	0.06	0.05	0.05
Winter	0.03	0.03	0.02	0.04	0.03	0.03	0.04	0.04	0.03

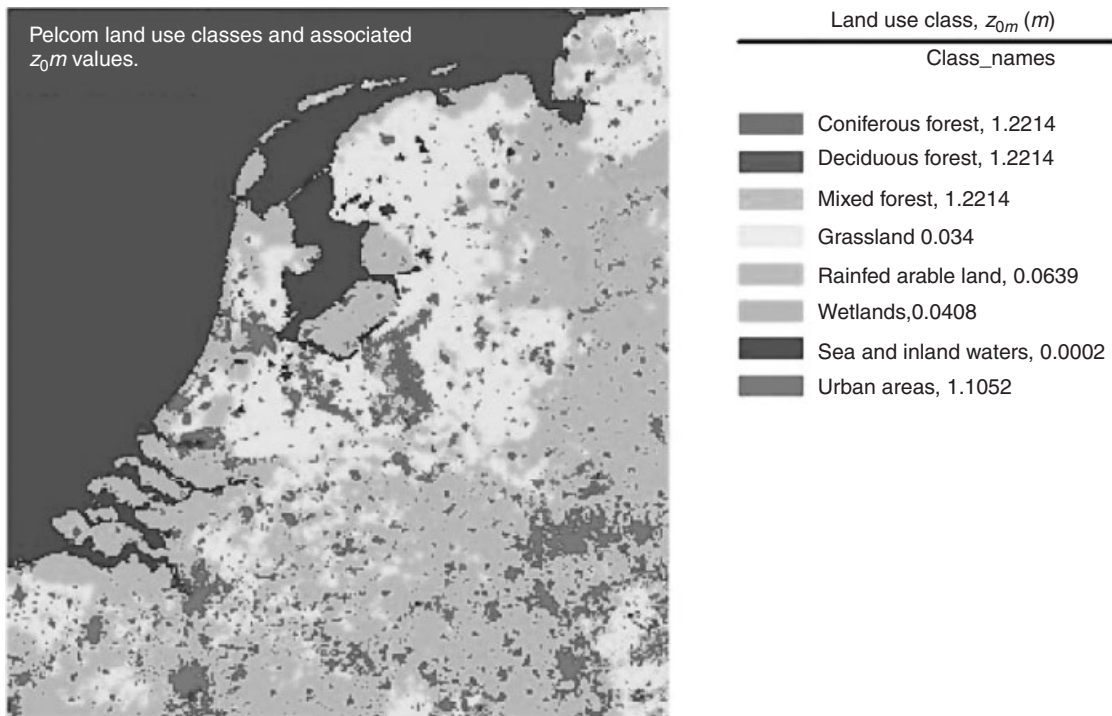


**Figure 5** A map of aerodynamic roughness height for the Netherlands based on land-use classes. A color version of this image is available at <http://www.mrw.interscience.wiley.com/ehs>

Sensing Satellite (ERS-2). In order to validate the effectiveness of the approach, three Large Aperture Scintillometers (LAS) providing line-averaged measurements of sensible heat flux over path lengths from 1 km to 5.2 km are used. The instruments were located far apart at three locations in Spain over different combinations of land cover and hydrological conditions and were operated continuously from April through September 1999. The LAS were installed at sites near Lleida, Badajoz, and Tomelloso (Figure 6). Each scintillometer site is additionally equipped with a shortwave radiometer to measure global radiation. Additional data that are necessary for the processing of LAS data were obtained from weather stations in the near surroundings.

The scintillometer near Lleida is installed in a region with small-scale irrigation at an altitude of 130 m. Main crops are fruit trees (peaches) and alfalfa. The distance between transmitter and receiver is approximately 4690 m. Both receiver and transmitter are installed on a hill, on a tripod at a height of, respectively, 45 m and 39 m above the surface. Meteorological data are obtained from the meteorological station near Juneda ( $41^{\circ}33'N$   $0^{\circ}49.5'E$ ).

The Badajoz LAS is located in a region with large-scale irrigation (sprinkler irrigation) at an altitude of 168 m. Crops being grown are wheat, corn, alfalfa, lettuce, olives, beans, and tomatoes. The distance between transmitter and receiver is  $5250 \text{ m} \pm 200 \text{ m}$ . The receiver is installed on top of a hill on a house, 68 m above the surrounding terrain.

The transmitter is installed on a water tower, 56 m above the surrounding terrain. Meteorological data are obtained from a station with short grass ground cover some 7 km from the LAS receiver.

The landscape of the Tomelloso site comprises a nearly level, alluvial floodplain to the north and a tilted old alluvial plain to the south. The vegetation consists of nonirrigated vineyards and a few olive orchards. The vines are broadly spaced and trellises are not used. The distance between transmitter and receiver is  $1070 \text{ m} \pm 40 \text{ m}$ . Both receiver and transmitter are installed on a steel mast at a height of, respectively, 4.15 m and 4.56 m above the surface at an altitude of 670 m. Meteorological data are obtained from a meteorological station near Tomelloso ( $39^{\circ}10'29.22''N$ ,  $3^{\circ}0'2.16''W$ ). Ground cover of the station is bare soil and grass. Longwave and shortwave radiation data, both incoming and outgoing, are available from this meteorological station.

Sensible heat flux  $H$  is calculated using SEBS at the ATSR passing time for corresponding days at each experimental site. The meteorological fields of wind, potential temperature, and humidity of air were generated by an advanced NWP model, the Regional Atmospheric Climate Model (RACMO) (Christensen *et al.*, 1996), integrated over the PBL. This implies that a single value of the reference wind, potential temperature, and humidity of air is used for each model grid, that is,  $25 \text{ km} \times 25 \text{ km}$ , while

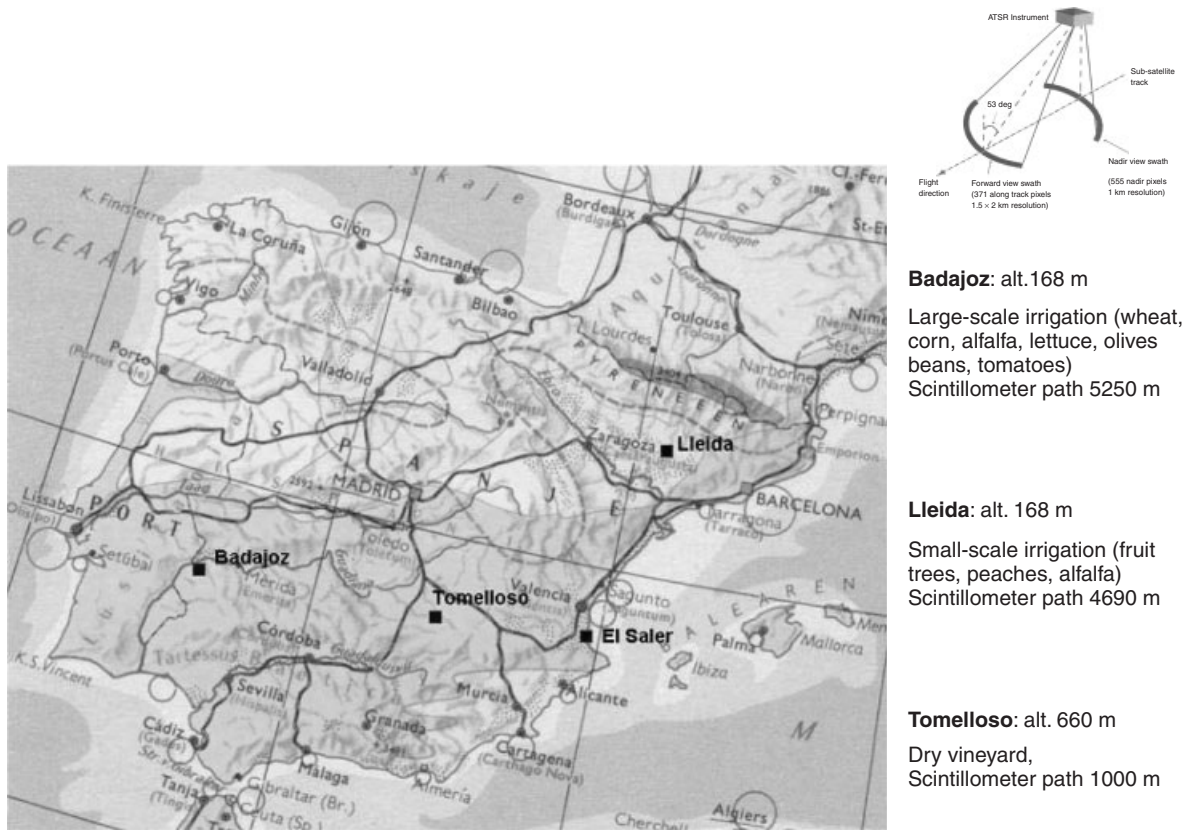


**Figure 6** Location of the three study sites in Spain (ATSR data plus meteorological data from nearest stations) and their characteristics. A color version of this image is available at <http://www.mrw.interscience.wiley.com/ehs>

the observations of vegetation properties have a resolution of  $1 \text{ km} \times 1 \text{ km}$  and account for sub-grid variability of land cover and hydrological conditions. The path lengths of the LAS measurements correspond to about five, six, and two ATSR pixels for the Lleida, Badajoz, and Tomelloso sites, respectively. The results from SEBS are quite comparable with the measurements as shown in Figure 7. In judging the validation results, it is important to keep the following issues in mind. First, the footprints in LAS measurements and in SEBS estimates are different. While the LAS-measured sensible heat flux is a line average along the path that only captures the contributions of turbulence from upwind direction over the averaging period, the SEBS estimates of sensible heat flux by using ATSR-measured surface variables and the NWP model-derived PBL variables are the average over a larger area, at least at ATSR pixel scale. Second, different temporal scales certainly contribute to the differences for the observed and estimated fluxes. Measurements from LAS are the mean values over 10 minutes, which represent the mixed turbulent characteristics and heat-exchange processes over the observation time, while a satellite only provides the instantaneous observations of surface variables at the satellite passing time. Moreover, if the surface shows large degree

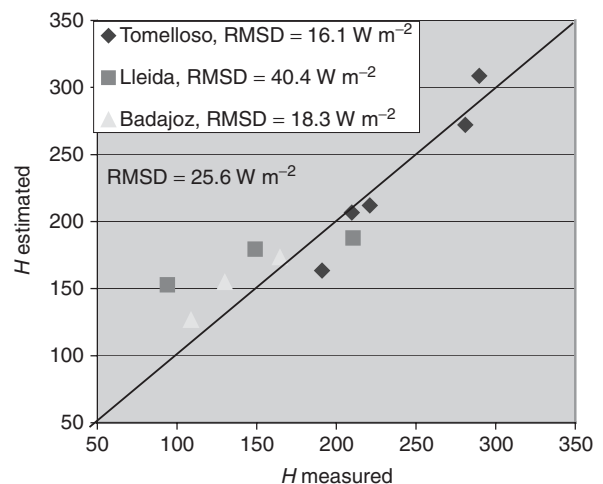


**Figure 7** Comparison of sensible heat flux values between SEBS and LAS measurements at the three experimental sites. A color version of this image is available at <http://www.mrw.interscience.wiley.com/ehs>

of heterogeneity, the determination of adequate pixels used to compare with the LAS-measured flux should be dealt with carefully.

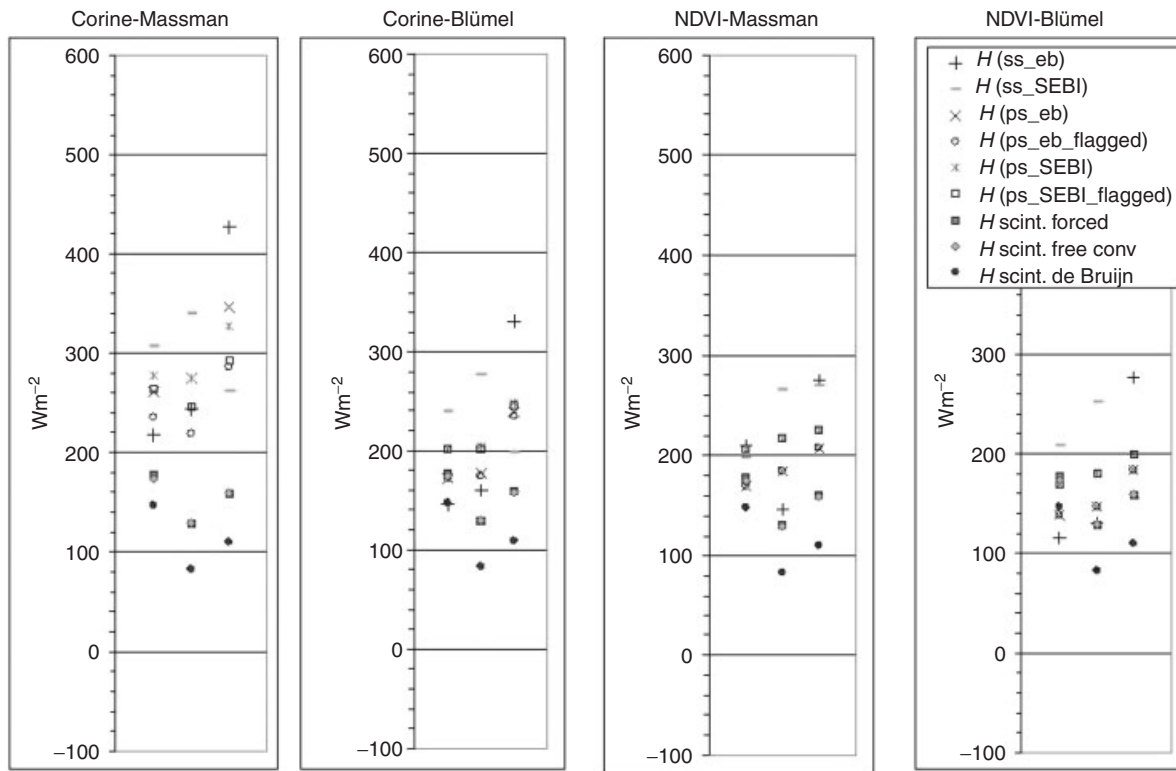


**Figure 8** Results derived from both single-source and parallel-source SEBS for Badajoz site (Corine refers to aerodynamic roughness derived from Corine land use map; Massman refers to the thermal dynamic roughness model of Su *et al.*, 2001; Blümel refers to the thermal dynamic roughness model of Blümel (1999); NDVI refers to aerodynamic roughness derived with NDVI – Normalized Difference Vegetation Index; ss – single source; ps – parallel source; eb – sensible heat flux derived from the nonlinear equations; sebi – sensible heat flux derived on the basis of the SEBI concept; flagged – energy limits are applied, that is, SEBS; scint, Forced. scint, Free convection. scint, de Bruin refer to three different ways of estimation of sensible heat fluxes from scintillometer measurements). A color version of this image is available at <http://www.mrw.interscience.wiley.com/ehs>

Further details about the measurements can be found in Moene and De Bruin (2001); Moene (2001). For details on the scintillometer method, the reader is referred to De Bruin (2002), and more details of the comparison can be found in Jia *et al.* (2003).

### Single-source SEBS versus Parallel-source SEBS

Essentially, the parameterization in single-source SEBS and parallel-source SEBS (see Figure 1 for details) are the same except in the case of the parallel-source SEBS, we first set the fractional cover of vegetation as unity and calculate the energy balance and turbulent heat-flux terms, then we do the same for soil by setting the fractional cover of soil as one, and finally we sum up the fluxes terms weighted by their actual fractional coverage.

Despite the simplicity of such a scheme, the results from the parallel-source SEBS are remarkably improved over the single-source SEBS as shown by Rauwerda *et al.* (2002) for three sites in Spain discussed above when the estimated

turbulent heat fluxes are compared to scintillometer measurements (see Figures 8, 9 and 10). The uncertainties caused by the different methods in determination of the roughness height for momentum are also amply demonstrated. It is also helpful to notice the differences in the LAS measurements derived from different processing methods. Further details on the comparison between single-source and parallel-source SEBS and ground measurements are given in Rauwerda *et al.* (2002).

### Some SEBS Applications to Water Sources Management

Besides the results presented above, SEBS has been used for several studies for water resources management conducted recently. Examples are estimation of actual evaporation in a semiarid inland basin in Northwest China (Li, 2001; Su *et al.*, 2003a) and drought disaster monitoring (Su *et al.*, 2003b).

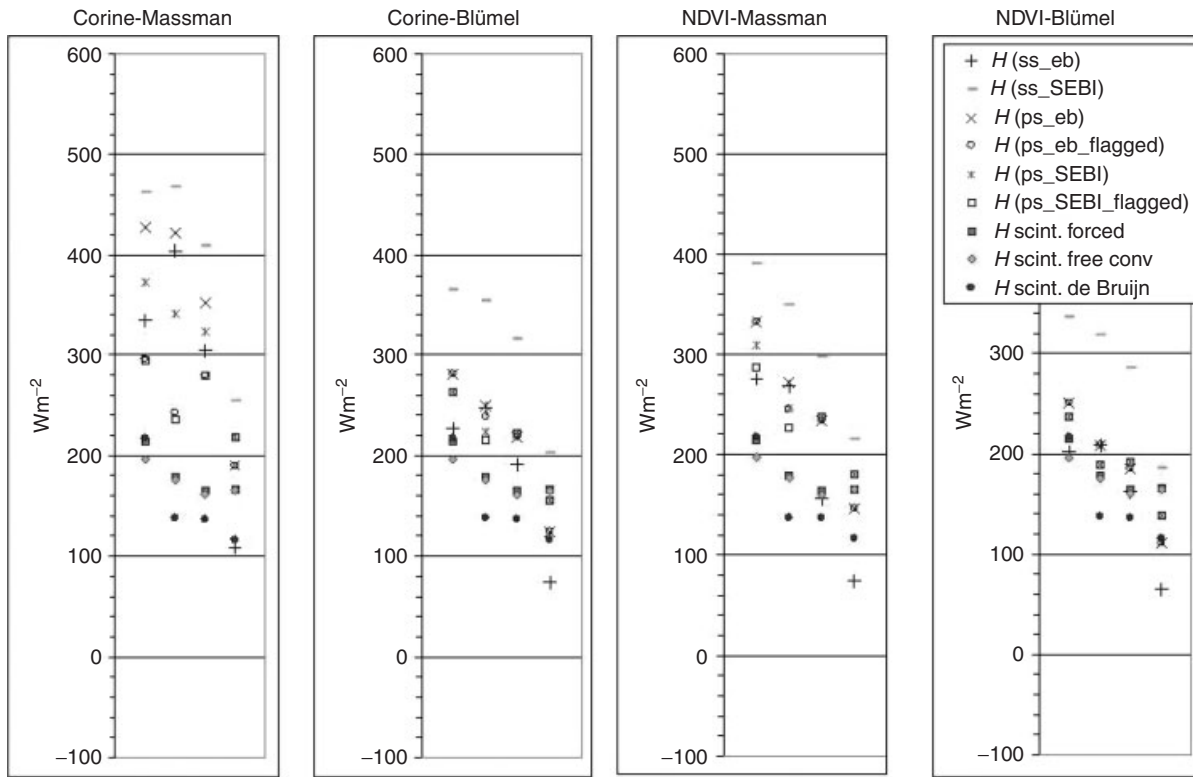


**Figure 9** Results derived from both single-source and parallel-source SEBS for Lleida site (explanation of symbols is the same as for in Figure 8). A color version of this image is available at <http://www.mrw.interscience.wiley.com/ehs>

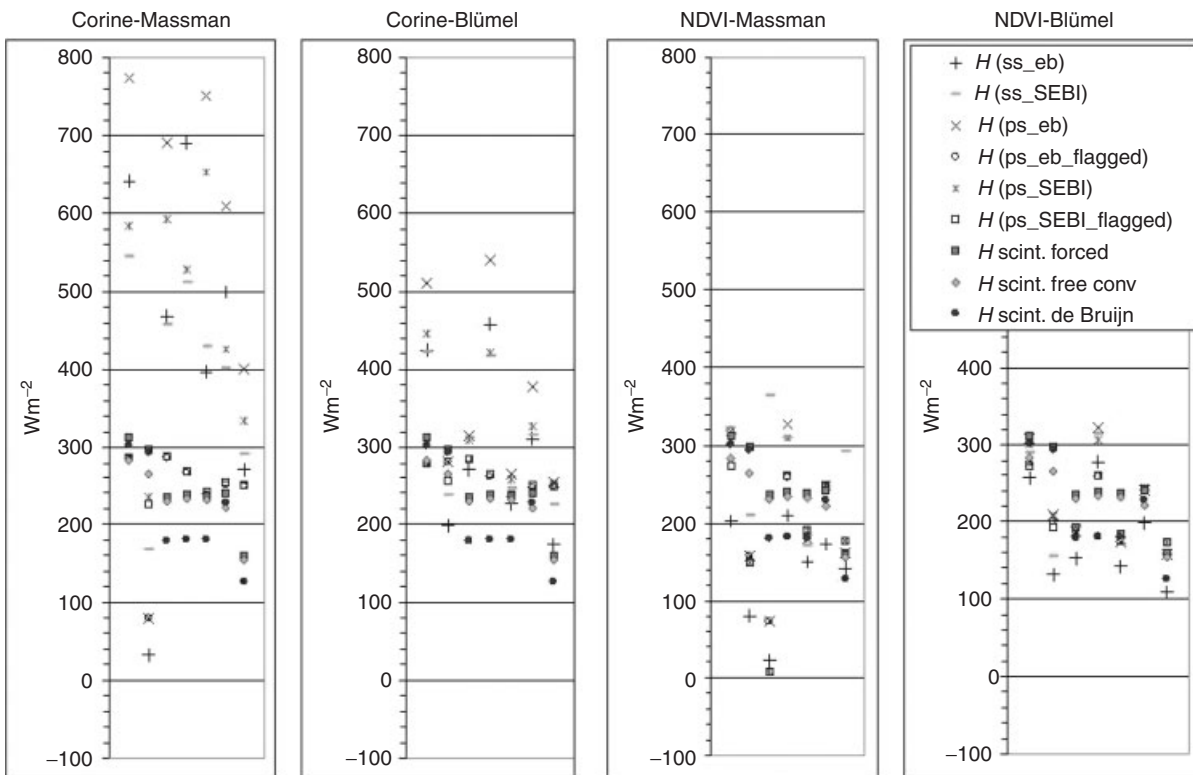


**Figure 10** Results derived from both single-source and parallel-source SEBS for Tomelloso site (explanation of symbols is the same as for in Figure 8). A color version of this image is available at <http://www.mrw.interscience.wiley.com/ehs>

### *Estimation of Actual Evaporation in the Urumqi River Basin*

SEBS is applied to Advanced Very High Resolution Radiometer (AVHRR) data for the estimation of actual evaporation in the Urumqi River Basin located in Xinjiang Uygur Autonomous Region in Northwest China. The Urumqi River Basin has all the features of a continental arid climate. Its diversity in topography offers a variety of land cover and vegetation. As such, the methodology and procedures developed for the Urumqi River Basin can be easily applied to other river basins in Northwest China and elsewhere in the world. Two water balance field experimental stations: Changji Station and Wulapo Station, equipped with routine meteorological instruments, evaporation pans of different sizes (E20, E60, and E5000), and lysimeters with different soils and vegetation types, provided sufficient information for calculation and verification. The size of the AVHRR data being processed for evaporation estimation was set between 86°38'E–88°59'E and 43°07'N–45°02'N, with a total area of about 27 800 km<sup>2</sup>. Hundred-and-five scenes in 1995 covering the basin were downloaded from Satellite Active Archive, among which 12 scenes were carefully chosen for evaporation calculation. Meteorological information is derived from the Changji meteorological station including wind speed (m/s), relative humidity, potential air temperature (K), and surface air pressure (Pa), and is scaled to PBL variables using the logarithmic profiles.

Verifications of the derived evaporation are performed by comparing with evaporation from different types of land surface collected in intensive field surveys for water resources assessment of the Urumqi River Basin (Li, 2001). Comparison between the annual evaporation derived from SEBS against the field measurements shows that the estimated values agree very well with the ground data except for the midmountainous area. The reason for the large relative error for the mountainous area could be due to the input of average elevation during the calculation as well as the uncertainty associated with the field information. More details on this case study can be found in Li (2001).

### *Application of SEBS in Drought Monitoring*

On the basis of SEBS, Su *et al.* (2003b) have proposed a method for assessing relative soil moisture with remote sensing data and have theoretically shown that the relative soil moisture in the rooting zone can be derived from relative evaporation. The relationship derived between the relative soil moisture and relative evaporation is confirmed with experimental data collected with lysimeter measurements in an eight-year-old orchard of peach trees (Girona *et al.*, 2002), and with measurements collected in an intensive field experiment in the Global Energy and Water Experiment (GEWEX) Asia Monsoon Experiment in Tibet (GAME/Tibet) in 1998 (Koike, 2000; Ma *et al.*, 2002). Further, it was shown that the proposed theory can be used to

define a Drought Severity Index (DSI) for drought monitoring, with the relative evaporation determined with remote sensing data. A demonstration for the latter was performed for North China in 2000 using remote sensing data AVHRR and routine meteorological data obtained from the operational measurement network of the National Meteorological Center of China. In the growing season with low rainfall, the value of DSI was high, and in the reverse case, the DSI value was low, which demonstrates that the DSI is in accordance with the data of rainfall in time and can be used to quantify drought situation both in temporal and spatial scales. Spatially, the derived DSI could identify that the central, the Northern, and then the Southern part of Shanxi province suffer under severe drought conditions in decreasing drought intensity in 2000. Temporarily, low soil water deficit was identified in July and August in most parts of Shanxi province. Higher soil water deficit occurred in April, May, and September 2000 with decreasing degree of intensity. Comparisons between the estimated relative evaporation and the actual measurements of soil moisture confirmed the general validity and robustness of the proposed method, but more extensive validation with field measurements at regional scale is considered necessary to quantify the accuracy of the proposed DSI method.

In all applications, benefits when using radiometric measurements are clearly demonstrated.

### **Using SEBS in a Data Assimilation System Environment**

A valuable first attempt in this direction has been made recently by Wood *et al.* (2003) who applied SEBS to the Southern Great Plains (SGP) region of the United States where the Atmospheric Radiation Measurement (ARM) program is carried out by the US Department of Energy. Energy Balance Bowen Ratio (EBBR) and Soil Water And Temperature System (SWATS) are also available at many ARM/Cloud And Radiation Testbed (CART) stations, and provide measurements of surface latent, sensible, and ground heat fluxes, as well as soil moisture and soil temperature. The surface meteorology used in SEBS is retrieved from the Eta Data Assimilation System (EDAS), while the solar radiation was processed by National Oceanic and Atmospheric Administration (NOAA/NESDIS) as part of the North American Land Data Assimilation System (NLDAS) (Mitchell *et al.*, 1999). The temperature product from the Moderate-Resolution Imaging Spectroradiometer (MODIS) on the Earth Observation Satellite (EOS) Terra was used to estimate the land surface temperature across the domain.

Measurements from the EBBR sites were compared with model-derived latent heat fluxes. For the 40 clear-sky days, an areal average instantaneous flux was calculated across the nine EBBR sites from the collocated SEBS pixels, with observations approximately 20% less than predictions.

**Table 3** Statistics of estimated versus observed heat fluxes of the Cotton dataset of Kustas (1990) with different algorithms (Root mean-squared difference between estimated and measured fluxes ( $Wm^{-2}$ ))

Method & reference	$R_n$	$G_0$	$H$	$\lambda E$	No. of observations
Observed mean value ( $W m^{-2}$ )	561.74	140.37	116.63	304.74	19
RMSD for SEBS (Su, 2002, Table 1)	22.82	5.42	21.22	29.22	19
RMSD for Two-source model (Kustas and Norman, 1999, Table 3)	19	18	23	42	19
RMSD for Two-source model (Kustas and Norman, 1999, Table 4)	21	13	25	37	19
RMSD for Two-source model (Kustas and Norman, 1999, Table 5)	20	10	36	47	19

Such differences may be attributed to the uncertainties in SEBS, especially in the roughness parameterization as discussed previously, but may similarly be attributed to uncertainties in surface flux measurements, because comparisons among different measurement setups may easily produce discrepancies of up to 25% (e.g. Twine *et al.*, 2000). While there exists a systematic overprediction in the SEBS/MODIS estimates when compared to the EBBR data, the results are encouraging and indicate that the SEBS approach has promise in estimating surface heat flux from space for data assimilation purposes.

### Results for SEBS and Other Techniques When Applied to Experimental Data Sets

In order to assess the accuracy of SEBS in comparison with some other techniques, results obtained with the same experimental data sets will be briefly discussed. Three field datasets obtained from flux stations that have been used extensively to benchmark surface energy balance algorithms (e.g. Norman *et al.*, 1995; Zhan *et al.*, 1996; Kustas and Norman, 1999; Su *et al.*, 2001; Su, 2002) will be used as examples. These three datasets are the Cotton dataset of Kustas (1990), the Shrub, and the Grass dataset of Kustas *et al.* (1994).

For the application of SEBS, the aerodynamic parameters are the model estimates as discussed in Su (2003). All other input variables are measured except the downward long-wave radiation that is estimated with the Stefan-Boltzmann radiation equation with the measured air temperature at the reference height. The parameterization used in SEBS is meant to be site-independent and, therefore, there is no site-specific adjustment or optimization involved. The details of the application of the other techniques are given in Kustas and Norman (1999) and Zhan *et al.* (1996) with some different site-specific parameterizations involved. The latter has evaluated four different techniques using the same data sets.

Table 3 shows the statistics of estimated versus observed heat fluxes of the Cotton dataset of Kustas (1990) with SEBS and the two-source model of Norman *et al.* (1995) using three different parameterizations (Kustas and Norman, 1999). Given the observed mean values of the net radiation, soil heat flux, sensible heat flux, and latent heat flux, the uncertainties of the estimated values (here expressed as the ratio of the root mean squared difference (RMSD) between the estimated and the observed values) are all within 20% of the mean observed values, except the sensible heat flux for the last row, which reaches 30% of uncertainty. The higher uncertainty in the latter case was due to the use of explicit soil and vegetation component temperatures and might be considered as an indication that the used two-source model needs some modification in order to be able to take advantage of the availability of the component temperatures. It should be noticed that an uncertainty of 20% or less in the estimated turbulent heat fluxes represents the best case that can be achieved given the uncertainties in all the involved parameters and variables in the algorithms as well as the uncertainties in the measured turbulent heat fluxes. More details on the uncertainty analysis can be found in Su (2002).

Tables 4 and 5 display the statistics of estimated versus observed heat fluxes of the Shrub and the Grass dataset of Kustas *et al.* (1994) for SEBS and four different algorithms, including the two-source model of Norman *et al.* (1995). The accuracy of SEBS are comparable to the best case analyzed by Zhan *et al.* (1996), who only reported the statistics for the sensible heat fluxes estimated with the four different algorithms. It is worthwhile to point out that while in SEBS all the available data in the two datasets are used (320 and 281 observations, respectively), the application of the four other algorithms were restricted to well-developed unstable atmospheric surface layer by excluding the more problematic transitions periods and night-time observations (114 and 103 observations, respectively).

**Table 4** Statistics of estimated versus observed heat fluxes of the Shrub dataset of Kustas *et al.* (1994) with different algorithms (Root mean-squared difference between estimated and measured fluxes ( $W m^{-2}$ ))

Method (Reference)	$R_n$	$G_0$	$H$	$\lambda E$	No. of observations
SEBS (Su, 2002, Table 2)	35.11	46.29	28.61	82.79	320
Single-source model of Kustas <i>et al.</i> (1989) (Zhan <i>et al.</i> , 1996, Table 6)	–	–	33	–	114
Single-source model of Troufleau <i>et al.</i> (1997) (Zhan <i>et al.</i> , 1996, Table 6)	–	–	48	–	114
Dual-source model of Lhomme <i>et al.</i> (1994) (Zhan <i>et al.</i> , 1996, Table 6)	–	–	52	–	114
Dual-source model of Norman <i>et al.</i> (1995) (Zhan <i>et al.</i> , 1996, Table 6)	–	–	33	–	114

**Table 5** Statistics of estimated versus observed heat fluxes of the Grass dataset of Kustas *et al.* (1994) with different algorithms (Root mean-squared difference between estimated and measured fluxes ( $W m^{-2}$ ))

Method (Reference)	$R_n$	$G_0$	$H$	$\lambda E$	No. of observations
SEBS (Su, 2002, Table 3)	41.26	42.95	36.19	61.34	281
Single-source model of Kustas <i>et al.</i> (1989) (Zhan <i>et al.</i> , 1996, Table 7)	–	–	41	–	103
Single-source model of Troufleau <i>et al.</i> (1997) (Zhan <i>et al.</i> , 1996, Table 7)	–	–	33	–	103
Dual-source model of Lhomme <i>et al.</i> (1994) (Zhan <i>et al.</i> , 1996, Table 7)	–	–	124	–	103
Dual-source model of Norman <i>et al.</i> (1995) (Zhan <i>et al.</i> , 1996, Table 7)	–	–	34	–	103

From the above evaluations, it might be concluded that SEBS can be applied to different sites and different atmospheric stability situations while maintaining the same parameterizations. This might prove important and critical when application to large scale is desired where no sufficiently detailed information on the site characteristics or the local atmospheric stability regime is available.

## DISCUSSION AND CONCLUSIONS

In this article, a brief introduction in estimation of radiation and turbulent heat fluxes using radiometric observations is given. In general, after the derivation of sensible heat flux, it is possible to estimate the latent heat flux as a residual by means of the energy balance equation, as was done in many other studies (e.g. Kalma and Jupp, 1990). However, the associated uncertainty in the derived latent heat flux and consequently in the evaporative fraction is large. This is because the sensible heat flux is, under given surface

conditions, determined solely by the surface temperature and the meteorological conditions at the reference height and is not constrained by the available energy. If the surface temperature or the meteorological variables have large uncertainty, a straight propagation of such uncertainty into the resultant latent heat flux and evaporative fraction cannot be avoided. In the SEBS formulation, this uncertainty is limited by consideration of the energy balance at the limiting cases, because the actual sensible heat flux is constrained in the range set by the sensible heat flux at the wet limit derived from a combination equation, and the sensible heat flux at the dry limit set by the available energy. In this aspect, SEBS is similar to previous algorithms that estimate relative evaporation by means of an index (e.g. the CWSI) using a combination equation (Jackson *et al.*, 1981, 1988; Menenti and Choudhury, 1993; Moran *et al.*, 1994). However, none of these previous algorithms incorporated explicitly the formulation of the roughness height for heat transfer, instead they used fixed values. Since the roughness height for heat transfer can vary with geometrical

and environmental variables in several orders of magnitude for different surface types, this ignorance has been shown by several studies to cause great uncertainties in estimation of heat fluxes or evaporation using radiometric temperature measurements (e.g. Verhoef *et al.*, 1997; Su *et al.*, 2001). Although it is possible to calibrate these algorithms such that their estimates reproduce observations at local scale, it would be very difficult to extend them to regional/continental studies by means of satellite observations. These shortcomings are avoided in SEBS. In addition, the application of SEBS does not require any *a priori* knowledge of the actual turbulent heat fluxes, indicating that SEBS is a credible and independent approach. Due to this property, SEBS results may be used for validation and initialization of hydrological, atmospheric, and ecological models that usually require proper partition of the sensible and latent heat flux at different scales. SEBS results can also be used *via* data assimilation in the above models to increase the reliability of the model simulations and predictions. Another valuable approach would be to implement the representation of surface flux exchanges as described in SEBS into a data assimilation system for assimilating remote-sensing data using modern data assimilation techniques. Some initial encouraging attempts have been made recently by Jia *et al.* (2003) and Wood *et al.* (2003) in this direction.

The examples on the use of parallel-source SEBS clearly indicate the benefit to be gained when more detailed measurements of the state of the land surface can be made. Currently, it has been possible to separate several important variables into their components, for example, the temperature of soil and that of vegetation using currently available sensors (e.g. ATSR and AATSR – the Advanced ATSR on the ENVISAT satellite). By means of multidirectional and multispectral to hyperspectral measurements, it would also be possible to derive more detailed component variables, for example, the temperature of soil and that of vegetation separately for sunlit and sun-shade portions using future available sensors. Use of these variables in algorithms will enable much detailed description of the physical processes involved in land–atmosphere interactions.

In summary, it may be stated that advances on improving parameterization and predictability of hydrological and earth system models, in particular, physically based distributed models, will heavily rely on the understanding of physical processes at different scales as well as the ability to obtain distributed physical information, satellite earth observation will prove of paramount importance in the future. Understanding and quantification of radiation and latent and sensible heating through quantitative remote sensing may hold the key to understand the interaction of terrestrial ecosystems and the hydrological cycles from local to global scales, and as such shall meet the challenges

in research and applications in areas ranging from numerical weather forecast, climate research, water cycle study, to water resources management, sustainable agricultural production, and ecological conservation.

### Acknowledgments

Researches leading to the work presented here were jointly funded by the Dutch Remote Sensing Board (BCRS), the Dutch Ministry of Agriculture, Nature Management, and Fisheries (LNV), and the Royal Netherlands Academy of Science (KNAW). The author has benefited greatly from discussion and debates with many colleagues. In particular, assistance and constructive comments from Li Jia, Jun Wen, Han Rauwerda, Gerbert Roerink, Katja Sintonen and Claire Jacobs (Alterra), Massimo Menenti and Zhao-Liang Li (TRIO/ULP), Bart van den Hurk (KNMI), Jieming Wang and Yaoming Ma (CAREER/CAS), Henk de Bruin and Arnold Moene (WU), Renhua Zhang and Xiaoming Sun (IGSNRR/CAS), Xiaomei Li and Li Wan (China University of Geosciences), Tom Schmutge and Bill Kustas (USDA/ARS), Bill Massman (USDA/FS), Wilfried Brutsaert (Connell University), Jetse Kalma (The University of Newcastle) and Eric Wood (Princeton University) are gratefully appreciated.

### REFERENCES

- Bastiaanssen W.G.M. (1995) *Regionalization of Surface Flux Densities and Moisture Indicators in Composite Terrain – A Remote Sensing Approach Under Clear Skies in Mediterranean Climates*, Ph.D. thesis, Wageningen Agricultural University, The Netherlands, p. 273.
- Beljaars A.C.M. and Bosveld F.C. (1997) Cabauw data for the validation of land surface parameterization schemes. *Journal of Climate*, **10**, 1172–1193.
- Beljaars A.C.M. and Holtslag A.A.M. (1991) Flux parameterization over land surfaces for atmospheric models. *Journal of Applied Meteorology*, **30**, 327–341.
- Blümel K. (1999) A simple formula for estimation of the roughness length for heat transfer over partly vegetated surfaces. *Journal of Applied Meteorology*, **38**, 814–829.
- Boegh E., Soegaard H. and Thomsen A. (2002) Evaluating evapotranspiration rates and surface conditions using Landsat TM to estimate atmospheric resistance and surface resistance. *Remote Sensing of Environment*, **79**, 329–343.
- Boni G.D., Castelli F. and Entekhabi D. (2001b) Sampling strategies and assimilation of ground temperature for the estimation of surface energy fluxes. *IEEE Transactions on Geoscience Remote Sensing*, **39**, 165–172.
- Boni G.D., Entekhabi D. and Castelli F. (2001a) Land data assimilation with satellite measurements for the estimation of surface energy balance components and surface control of evaporation. *Water Resources Research*, **37**, 1713–1722.
- Bowen I.S. (1926) The ratio of heat losses by conduction and by evaporation from any water surface. *Physical Review*, **27**, 779–787.

- Brutsaert W. (1982) *Evaporation into the Atmosphere*, D. Reidel: Dordrecht.
- Brutsaert W. (1999) Aspects of bulk atmospheric boundary layer similarity under free-convective conditions. *Reviews of Geophysics*, **37**, 439–451.
- Campbell G.S. and Norman J.M. (1998) *An Introduction to Environmental Biophysics*, Springer.
- Caparrini F., Castelli F. and Entekhabi D. (2003) Mapping of land-atmosphere heat fluxes and surface parameters with remote sensing data. *Boundary-Layer Meteorology*, **107**, 605–633.
- Caparrini F., Castelli F. and Entekhabi D. (2004) Estimation of surface turbulent fluxes through assimilation of radiometric surface temperature sequences. *Journal of Hydrometeorology*, **5**, 145–159.
- Carlson T.N., Taconet O., Vidal A., Cillies R.R., Olioso A. and Humes K. (1995) An overview of the workshop on the thermal remote sensing held at La Londe les Maures, France, September 20–24, 1993. *Agricultural and Forest Meteorology*, **77**, 141–151.
- Castelli F., Entekhabi D. and Caporali E. (1999) Estimation of surface heat flux and an index of soil moisture using adjoint-state surface energy balance. *Water Resources Research*, **35**, 3115–3125.
- Chanzy A., Bruckler L. and Perrier A. (1995) Soil evaporation monitoring: a possible synergism of microwave and infrared remote sensing. *Journal of Hydrology*, **165**, 235–259.
- Chehbouni A., Nouvellon Y., Lhomme J.P., Watts C., Boulet G., Kerr Y.H., Moran M.S. and Goodrich D.C. (2001) Estimation of surface sensible heat flux using dual angle observations of radiative surface temperature. *Agricultural and Forest Meteorology*, **108**, 55–65.
- Choudhury B.J. and Monteith J.L. (1988) A four layer model for the heat budget of homogeneous land surfaces. *The Quarterly Journal of Royal Meteorological Society*, **114**, 373–398.
- Christensen J.H., Christensen O.B., Lopez P., Van Meijgaard E. and Botzet M. (1996) The HIRHAM4 Regional Atmospheric Climate Model, Scientific Report 96-4, Danish Meteorological Institute, Copenhagen, Scientific Report, 51.
- Crago R.D. (1996) Comparison of the evaporative fraction and the Priestley-Taylor a for parameterizing daytime evaporation. *Water Resources Research*, **32**(5), 1403–1409.
- De Bruin H.A.R. (2002) Renaissance of scintillometry. *Boundary Layer Meteorology*, **105**, 1–4.
- Entekhabi D., Asrar G.R., Betts A.K., Beven K.J., Bras R.L., Duffy C.J., Dunne T., Koster R.D., Lettenmaier D.P., McLaughlin D.B., et al. (1999) An agenda for land surface hydrology research and a call for the second international hydrological decade. *Bulletin of the American Meteorological Society*, **80**(10), 2043–2058.
- Famiglietti J.S. and Wood E.F. (1994) Multiscale modeling of spatially variable water and energy balance processes. *Water Resources Research*, **30**, 3061–3078.
- Girona J., Mata M., Fereres E., Goldammer D.A. and Cohen M. (2002) Evapotranspiration and soil water dynamics of peach trees under water deficits. *Agricultural Water Management*, **54**, 107–122.
- Hasager C. and Jensen N.O. (1999) Surface-flux aggregation in heterogeneous terrain. *The Quarterly Journal of Royal Meteorological Society*, **125**, 1–28.
- Högström U. (1988) Non-dimensional wind and temperature profiles in the atmospheric surface layer: a re-evaluation. *Boundary-Layer Meteorology*, **42**, 55–78.
- Iqbal M. (1983) *An Introduction to Solar Radiation*, Academic Press: Toronto.
- Jackson R.D., Idso S.B., Reginato R.J. and Pinter P.J. Jr (1981) Canopy temperature as a crop water stress indicator. *Water Resources Research*, **17**(4), 1133–1138.
- Jackson R.D., Kustas W.P. and Choudhury B.J. (1988) A re-examination of the crop water stress index. *Irrigation Science*, **9**, 309–317.
- Jackson R.D., Reginato R.J. and Idso S.B. (1977) Wheat canopy temperature: A practical tool for evaluating water requirements. *Water Resources Research*, **13**, 651–656.
- Jia L., Menenti M., Su Z., Djepa V., Li Z.-L. and Wang J. (2001) Modeling sensible heat flux using estimates of soil and foliage temperatures: the HEIFE and IMGRASS experiments. In *Remote Sensing and Climate Modeling: Synergies and Limitations*, Beniston M. and Verstraete M. (Eds.), Kluwer Academic Publisher: Dordrecht.
- Jia L., Su Z., van den Hurk B., Menenti M., Moene A., De Bruin H.A.R., Yrisarry J.J.B., Ibanez M. and Cuesta A. (2003) Estimation of sensible heat flux using the surface energy balance system (SEBS) and ATSR measurements. *Physics Chemistry of the Earth*, **28**(1–3), 75–88.
- Kabat P. (1999) *The Role of Biospheric Feedbacks in the Hydrological Cycle*, The IGBP – BAHC Special Issue, (Global Change Newsletter), IGBP Newsletter, 39.
- Kader B.A. and Yaglom A.M. (1990) Mean fields and fluctuation moments in unstably stratified turbulent boundary layers. *Journal of Fluid Mechanics*, **212**, 637–662.
- Kalma J.D. and Jupp D.L.B. (1990) Estimating evaporation from pasture using infrared thermometry: evaluation of a one-layer resistance model. *Agricultural and Forest Meteorology*, **51**, 223–246.
- Kalnay E. and Cai M. (2003) Impact of urbanization and land-use change on climate. *Nature*, **423**, 528–531.
- Katul G.G. and Parlange M.B. (1992) A Penman-Brutsaert model for wet surface evaporation. *Water Resources Research*, **28**(1), 121–126.
- Koike T. (2000) The overview of GAME/Tibet. *Proceedings of The Second Session of International Workshop on TIPEX-GAME/Tibet*, Kunming, July 20–22, 2000.
- Koster R.D., Suarez M.J. and Heiser M. (2000) Variance and predictability of precipitation at seasonal to interannual timescale. *Journal of Hydrometeorology*, **1**, 26–46.
- Kustas W.P. (1990) Estimates of evapotranspiration with a one and two layer model of heat transfer over partial canopy layer. *Journal of Applied Meteorology*, **29**, 704–715.
- Kustas W.P., Blanford J.H., Stannard D.I., Daughtry C.S.T., Nichols W.D. and Weltz M.A. (1994) Local energy flux estimates for unstable conditions using variance data in semiarid rangelands. *Water Resources Research*, **30**, 1351–1361.
- Kustas W.P. and Daughtry C.S.T. (1989) Estimation of the soil heat flux/net radiation ratio from spectral data. *Agricultural and Forest Meteorology*, **49**, 205–223.
- Kustas W.P. and Norman J.M. (1996) Use of remote sensing for evapotranspiration monitoring over land surfaces. *Hydrological Sciences Journal*, **41**(4), 495–516.

- Kustas W.P. and Norman J.M. (1999) Evaluation of soil and vegetation heat flux predictions using a simple two-source model with radiometric temperatures for partial canopy cover. *Agricultural and Forest Meteorology*, **94**, 13–29.
- Lhomme J.-P., Monteny B. and Amadou M. (1994) Estimating sensible heat flux from radiometric temperature over sparse millet. *Agricultural and Forest Meteorology*, **68**, 77–91.
- Li X. (2001) *Estimation of Urumqi River Basin Evaporation with Remote Sensing*, M.Sc. Thesis in Hydrological Engineering, UNESCO-IHE, Delft.
- Ma M., Su Z., Li Z.-L., Koike T. and Menenti M. (2002) Determination of regional net radiation and soil heat flux over a heterogeneous landscape of the Tibetan Plateau. *Hydrological Processes*, **16**(15), 2963–2971.
- Massman W.J. (1997) An analytical one-dimensional model of momentum transfer by vegetation of arbitrary structure. *Boundary-Layer Meteorology*, **83**, 407–421.
- Massman W.J. (1999a) A model study of  $kB_H^{-1}$  for vegetated surfaces using 'localized near-field' Lagrangian theory. *Journal of Hydrology*, **223**, 27–43.
- Massman W.J. (1999b) Molecular diffusivities of Hg vapor in air, O<sub>2</sub> and N<sub>2</sub> near STP and the kinematic viscosity and the thermal diffusivity of air near STP. *Atmospheric environment*, **33**, 453–457.
- Mecikalski J.M., Diak G.R., Anderson M.C. and Norman J.M. (1999) Estimating fluxes on continental scales using remotely-sensed data in an atmosphere-land exchange model. *Journal of Applied Meteorology*, **38**, 1352–1369.
- Menenti M. (1984) *Physical Aspects of and Determination of Evaporation in Deserts Applying Remote Sensing Techniques*, Report 10 (special issue), Institute for Land and Water Management Research (ICW): The Netherlands.
- Menenti M. (1993) Understanding land surface evapotranspiration with satellite multispectral measurements. *Advances in Space Research*, **13**(5), 89–100.
- Menenti M. and Choudhury B.J. (1993) Parameterization of land surface evapotranspiration using a location-dependent potential evapotranspiration and surface temperature range. In *Exchange Processes at the Land Surface for a Range of Space and Time Scales*, Bolle H.J., Feddes R.A. and Kalma J.D. (Eds.), IAHS Publication No. 212: 561–568.
- Menenti M., Choudhury B.J. and Di Girolamo N. (2001) Monitoring of actual evaporation in the Aral Basin using AVHRR observations and 4DDA results. In *Advanced Earth Observation – Land Surface Climate*, Su Z. and Jacobs C. (Eds.), Report USP-2, 01–02, Publications of the National Remote Sensing Board (BCRS): pp. 79–83.
- Menenti M. and Ritchie J.C. (1994) Estimation of effective aerodynamic roughness of Walnut Gulch watershed with laser altimeter measurements. *Water Resources Research*, **30**, 1329–1337.
- Mitchell K., Houser P., Wood E., Schaake J., Tarpley D., Lettenmaier D., Higgins W., Marshall C., Lohmann D., Ek M., et al. (1999) GCIIP land data assimilation system (LDAS) project now underway, *GEWEX News*, **9**(4), 3–6.
- Moene A.F. (2001) Description of field experiments. In *Advanced Earth Observation – Land Surface Climate*, Su Z. and Jacobs C. (Eds.), Report USP-2, 01–02, Publications of the National Remote Sensing Board (BCRS).
- Moene A.F. and De Bruin H.A.R. (2001) Sensible heat flux data derived from the scintillometers. In *Advanced Earth Observation – Land Surface Climate*, Su Z. and Jacobs C. (Eds.), Report USP-2, 01–02, Publications of the National Remote Sensing Board (BCRS).
- Monteith J.L. (1965) Evaporation and environment. *Symposia of the Society for Experimental Biology*, **19**, 205–234.
- Monteith J.L. (1973) *Principles of Environmental Physics*, Edward Arnold Press.
- Monteith J.L. (1981) Evaporation and Surface Temperature. *The Quarterly Journal of Royal Meteorological Society*, **107**, 1–27.
- Morton F.I. (1983) Operational estimates of areal evapotranspiration and their significance to the practice of hydrology. *Journal of Hydrology*, **66**, 1–76.
- Moran M.S., Clarke T.R., Inoue Y. and Vidal A. (1994) Estimating crop water deficit using the relation between surface-air temperature and spectral vegetation index. *Remote Sensing of Environment*, **49**, 246–263.
- Mücher C.A., Steinnocher K., Champeaux J.L., Griguolo S., Wester K. and Loudjani P. (2001) *Land Cover Characterization for Environmental Monitoring of Pan-Europe*, Wageningen University and Research Centre, Centre for Geo-information: Wageningen, <http://cgi.girs.wageningen-ur.nl/cgi/projects/eu/pelcom/public/index.htm>.
- Nieuwenhuis G.J.A., Schmidt E.A. and Tunnissen H.A.M. (1985) Estimation of regional evapotranspiration of arable crops from thermal infrared images. *International Journal of Remote Sensing Environment*, **6**, 1319–1334.
- Nishida K., Nemani R.R., Glassy J.M. and Running S.W. (2003a) Development of an evapotranspiration index from aqua/MODIS for monitoring surface moisture status. *IEEE Transactions on Geoscience Remote Sensing*, **41**(2), 493–501.
- Nishida K., Nemani R.R., Running S.W. and Glassy J.M. (2003b) An operational remote sensing algorithm of land surface evaporation, *Journal of Geophysical Research-Atmospheres*, **108**(D9), Art. No. 4270, doi:10.1029/2002JD002062.
- Norman J.M., Kustas W.P. and Humes K.S. (1995) A two-source approach for estimating soil and vegetation energy fluxes from observations of directional radiometric surface temperature. *Agricultural and Forest Meteorology*, **77**, 263–293.
- Olioso A., Braud I., Chanzy A., Demarty J., Ducros Y., Gaudu J.-C., Gonzalez-Sosa E., Lewan E., Marloie O., Ottle C., et al. (2002) Monitoring energy and mass transfers during the Alpillies-ReSeDA experiment. *Agronomie*, **22**, 597–610.
- Penman H.L. (1948) Natural evaporation from open water, bare soil and grass. *Proceedings of the Royal Society of London. Series A*, **193**, 120–146.
- Pielke R.A. Sr (2001a) Influence of the spatial distribution of vegetation and soils on the prediction of cumulus convective rainfall. *Reviews of Geophysics*, **39**, 151–177.
- Pielke R.A. Sr (2001b) Comments on IPCC report cautiously warns of potentially dramatic climate change impacts. *The Earth Observing System*, **82**, 394–396.
- Press W.H., Teukolsky S.A., Vetterling W.T. and Flannery B.P. (1997) *Numerical Recipes in C: The Art of Scientific Computing*, Cambridge University Press.
- Priestley C.H.B. and Taylor R.J. (1972) On the assessment of surface heat flux and evaporation using large-scale parameters. *Monthly Weather Review*, **100**(2), 81–92.

- Rauwerda J., Roerink G.J. and Su Z. (2002) *Estimation of Evaporative Fractions by the Use of Vegetation and Soil Component Temperatures Determined by Means of Dual-Looking Remote Sensing*, Alterra-report 580, ISSN 1566-7197.
- Roerink G.J., Su Z. and Menenti M. (2000) S-SEBI: A simple remote sensing algorithm to estimate the surface energy balance. *Physics Chemistry of the Earth*, **25**, 147–157.
- Seguin B. and Ittier B. (1983) Using midday surface temperature to estimate daily evaporation from satellite thermal IR data. *International Journal of Remote Sensing Environment*, **4**, 371–383.
- Sellers P.J., Randall D.A., Collatz G.J., Berry J.A., Field C.B., Dazlich D.A., Zhang C., Collelo G.D. and Nounoua L. (1996) A revised land surface parameterization (SiB2) for atmospheric GCMS, part 1: model formulation. *Journal of Climate*, **9**, 676–705.
- Shuttleworth W.J., Gurney R.J., Hsu A.Y. and Ormsby J.P. (1989) FIFE: the variation in energy partition at surface flux sites. *IAHS Publication*, **186**, 67–74.
- Shuttleworth W.J. and Wallace J.S. (1985) Evaporation from sparse crops – an energy combination theory. *The Quarterly Journal of Royal Meteorological Society*, **111**, 939–955.
- Stanghellini C. (1987) *Transpiration of Greenhouse Crops – an Aid to Climate Management*, Ph.D. thesis, Agriculture University, Wageningen.
- Stull R.B. (1988) *An Introduction to Boundary Layer Meteorology*, Kluwer Academic Publishers: Dordrecht.
- Su Z. (2002) The surface energy balance system (SEBS) for estimation of turbulent heat fluxes. *Hydrol. Earth Sys. Sci.*, **6**(1), 85–99.
- Su Z. and Jacobs C. (Eds.) (2001) *Advanced Earth Observation – Land Surface Climate*, Report USP-2, 01–02, Publications of the National Remote Sensing Board (BCRS).
- Su Z. and Menenti M. (Eds.) (1999) *Mesoscale Climate Hydrology: The Contribution of the New Observing Systems*, Report USP-2, 99-05, Publications of the National Remote Sensing Board (BCRS).
- Su Z., Li X., Zhou Y., Wan L., Wen J. and Sintonen K. (2003a) Estimating areal evaporation from remote sensing. *Paper Presented at the International Geoscience and Remote Sensing Symposium*, 21–25 July 2003, Toulouse (PID20349.pdf).
- Su Z., Pelgrum H. and Menenti M. (1999) Aggregation effects of surface heterogeneity in land surface processes. *Hydrology and Earth System Sciences*, **3**(4), 549–563.
- Su Z., Schmugge T., Kustas W.P. and Massman W.J. (2001) An evaluation of two models for estimation of the roughness height for heat transfer between the land surface and the atmosphere. *Journal of Applied Meteorology*, **40**(11), 1933–1951.
- Su Z., Yacob A., Wen J., Roerink G., He Y., Gao B., Boogaard H. and van Diepen C. (2003b) Assessing relative soil moisture with remote sensing data: theory and experimental validation. *Physics Chemistry of the Earth*, **28**(1–3), 89–101.
- Sugita M. and Brutsaert W. (1991) Daily evaporation over a region from lower boundary-layer profiles measured with radiosondes. *Water Resources Research*, **27**(5), 747–752.
- Troufleau D., Lhomme J.-P., Monteny B. and Vidal A. (1997) Sensible heat flux and radiometric temperature over sparse Sahelian vegetation I: An experimental analysis of the  $kB^{-1}$  parameter. *Journal of Hydrology*, **188–189**(1–4), 815–838.
- Twine T.E., Kustas W.P., Norman J.M., Cook D.R., Houser P.R., Meyers T.P., Prueger J.H., Starks P.J. and Wesley M.L. (2000) Correcting eddy-covariance flux underestimates over a grassland. *Agricultural and Forest Meteorology*, **103**, 279–300.
- Van den Hurk B.J.J.M. and Holtslag A.A.M. (1995) On the bulk parameterization of surface fluxes for various conditions and parameter ranges. *Boundary-Layer Meteorology*, **82**, 199–234.
- Verhoef A., de Bruin H.A.R. and van den Hurk B.J.J.M. (1997) Some practical notes on the parameter for sparse vegetation. *Journal of Applied Meteorology*, **36**, 560–572.
- Wieringa J. (1993) Representative roughness parameters for homogeneous terrain. *Boundary-Layer Meteorology*, **63**, 323–363.
- Wood E.F. (1998) *Hydrologic Measurements and Observations: an Assessment of Needs in Hydrologic Sciences: Taking Stock and Looking Ahead*, National Academy Press, pp. 67–86.
- Wood E.F., Su H., McCabe M. and Su Z. (2003) Estimating evaporation from satellite remote sensing. Paper presented at the *International Geoscience and Remote Sensing Symposium*, 21–25 July 2003, Toulouse (PID20004.pdf).
- Zhan X., Kustas W.P. and Humes K.S. (1996) An intercomparison study on models of sensible heat flux over partial canopy surfaces with remotely sensed surface temperature. *Remote Sensing of Environment*, **58**, 242–256.
- Zhang R.H. (1996) *Remote Sensing Models and Ground Surface Foundation*, The Science Press: Beijing.